Cardiac Muscarinic Receptors. Cooperativity as the Basis for Multiple States of Affinity†

Peter Chidiac,‡ Marty A. Green, Asha B. Pawagi, and James W. Wells*

Department of Pharmacology and Faculty of Pharmacy, University of Toronto, Toronto, Ontario, Canada M5S 2S2

Received August 5, 1996; Revised Manuscript Received February 24, 1997⊗

ABSTRACT: Cooperativity has been investigated as the mechanistic basis for effects observed with cardiac muscarinic receptors in washed membranes from Syrian hamsters. Specifically, *N*-[^{3}H]methylscopolamine labeled only 66−75% of the sites labeled by [^{3}H]quinuclidinylbenzilate at apparently saturating concentrations of each radioligand. Also, receptors labeled by *N*-[^{3}H]methylscopolamine revealed three states of affinity for agonists, both in native membranes and following irreversible blockade of about 80% of the sites by propylbenzilylcholine mustard; in both preparations, guanylylimidodiphosphate (GMP-PNP) effected an apparent interconversion of sites from higher to lower affinity for agonists and from lower to higher affinity for the antagonist. Excellent and mechanistically consistent descriptions of the data were obtained in terms of a model comprising cooperative and noncooperative forms of the receptor; the former was described by a variant of the Adair equation, and the latter was included to account for low-affinity sites that survived treatment with the mustard. If differences in apparent capacity derive from negative cooperativity in the binding of *N*-[^{3}H]methylscopolamine, the cooperative form of the receptor was at least trivalent in native membranes; otherwise, constraints imposed by the effects of GMP-PNP at the concentrations of radioligand used in the assays dictate that the cooperative form of the receptor was at least tetravalent. In contrast, a divalent receptor is sufficient with the data from alkylated membranes, in accord with the reduced likelihood of interactions between functional sites within an oligomeric array. A model is presented wherein the receptor interconverts spontaneously between two or more states differing in their cooperative properties. The effects of GMP-PNP can be rationalized as a shift in the equilibrium between the different states.

G protein-linked receptors reveal an intriguing but mechanistically ambiguous dispersion of affinities for agonists: quantitative measures of the dispersion correlate with efficacy or intrinsic activity [*e.g.*, Birdsall *et al.* (1977), Kent *et al.* (1980), Ehlert (1985), Evans *et al.* (1985), and Potter and Ferrendelli (1989)], but its underlying cause remains unclear. The effect is often attributed to heterogeneity induced by the G protein in an otherwise homogeneous population of mutually independent sites (De Lean *et al.*, 1980; Birnbaumer *et al.*, 1990). Such schemes suggest a mechanism for amplification of the neurohumoral signal, and they seem to account qualitatively for a wide range of biochemical and pharmacological effects, but they have fallen short in quantitative terms. They fail to describe the binding patterns in a mechanistically consistent manner, and their predictions conflict with other data on such properties as amplification, the relative numbers of receptors and G proteins, the effect of guanyl nucleotides, and the stability of the receptor−G protein complex (Wong *et al.*, 1986; Lee *et al.*, 1986; Wreggett, 1987; Ehlert and Rathbun, 1990; Graeser and Neubig, 1993; Green *et al.*, 1997).

There is a striking similarity between the effect of guanyl nucleotides on the binding of agonists to G protein-linked receptors and the effect of agonists on the binding of GDP to receptor-linked G proteins. Cardiac muscarinic receptors and their attendant G proteins exhibit multiple states for the agonist and the nucleotide, respectively, and either ligand favors those states of lower affinity for the other (Tota *et al.*, 1987; Hilf *et al.*, 1989; Chidiac and Wells, 1992; Green *et al.*, 1997). The reciprocal behavior suggests that binding is regulated by a single mechanism common to both sides, the ambiguity of the data notwithstanding.

In the presence of AMP-PNP, the specific binding of [^{35}S]-GTPγS to myocardial membranes has been found to exhibit a bell-shaped dependence on the concentration of GDP; also, the amplitude of the GDP-dependent increase was markedly greater in the presence of carbachol (Chidiac and Wells, 1992). A ligand-dependent increase in bound [^{35}S]GTPγS suggests that GDP and the radioligand bind to interacting sites and that the multiple states of affinity are a manifestation of cooperativity within an oligomeric array. A similar pattern has emerged with purified M_2 receptors associated with G_o and G_i in solubilized preparations from porcine atria, where the specific binding of [^{3}H]AF-DX 384 in the presence of GMP-PNP[1] revealed a bell-shaped dependence on the concentration of carbachol (Wreggett and Wells, 1995). Moreover, the apparent capacity of the preparation was higher for [^{3}H]quinuclidinylbenzilate than for [^{3}H]AF-DX

† This investigation was supported by the Heart and Stroke Foundation of Ontario, The Medical Research Council of Canada, and the Natural Sciences and Engineering Research Council of Canada.

* Author to whom correspondence should be addressed at the Faculty of Pharmacy, University of Toronto, 19 Russell St., Toronto, ON, Canada M5S 2S2 [telephone (416) 978-3068; fax (416) 978-8511; e-mail jwells@phm.utoronto.ca].

‡ Present address: Department of Pharmacology, Southwestern Medical Center, University of Texas, Dallas, TX 75235-9041.

⊗ Abstract published in *Advance ACS Abstracts,* May 15, 1997.

[1] Abbreviations: GMP-PNP, guanylylimidodiphosphate; HEPES, sodium *N*-(2-hydroxyethyl)piperazine-*N*′-2-ethanesulfonate; NMS, *N*-methylscopolamine.

S0006-2960(96)01939-3 CCC: $14.00

384 or *N*-[^{3}H]methylscopolamine, but specific binding of the former was fully inhibited by unlabeled analogues of the latter at anomalously low concentrations. All of the data could be described quantitatively in terms of cooperative effects among four interacting sites.

Evidence for such interactions represents a departure from the view that G protein-linked receptors function as mutually independent sites; also, the bell-shaped pattern reported for carbachol at purified M_2 receptors is atypical. To examine the implications of cooperativity under more commonly used conditions, a variant of the Adair equation has been assessed for its ability to describe the binding properties of cardiac muscarinic receptors in ventricular membranes. In this paper, the model is shown to provide a mechanistically consistent account of the data, including the binding of agonists and antagonists, the effects of GMP-PNP, the consequences of partial alkylation by propylbenzilylcholine mustard, and differences in the apparent capacity of the membranes for [^{3}H]quinuclidinylbenzilate and *N*-[^{3}H]methylscopolamine. In the accompanying paper, the data have been examined in terms of the alternative notion of heterogeneity induced by the G protein (Green *et al.*, 1997).

MATERIALS AND METHODS

Chemicals. (−)-[^{3}H]Quinuclidinylbenzilate (54.0 Ci/mmol) was purchased from DuPont NEN, and *N*-[^{3}H]-methylscopolamine chloride was purchased from DuPont NEN (85.0 Ci/mmol) and Amersham (74.0 Ci/mmol). Propylbenzilylcholine mustard was the gift of Dr. J. M. Young, Department of Pharmacology, University of Cambridge. Carbamylcholine chloride (carbachol), arecoline hydrobromide, methacholine chloride, and unlabeled *N*-methylscopolamine hydrobromide were purchased from Sigma Chemical Co. Methacholine was obtained as the racemate, and concentrations were calculated on the assumption that one isomer is inactive. Unlabeled guanyl nucleotides were purchased from Boehringer Mannheim. HEPES[1] was purchased as the free base from Calbiochem and from Boehringer Mannheim. Dithiothreitol and bacitracin were purchased from Sigma. EDTA was obtained as the free acid from British Drug Houses. All other chemicals were of reagent grade or better.

Preparation of Membranes. Adult Syrian golden hamsters were obtained from the breeding unit at the University of Toronto and from Harlan Sprague Dawley, Indianapolis, IN. The animals were killed by decapitation, the aorta was clamped, and the heart was injected via the left ventricle with an ice-cold solution containing sucrose (0.32 M), HEPES (20 mM), bacitracin (200 μg/mL), and EDTA (1.0 mM) adjusted to pH 7.45 with potassium hydroxide. The flushed heart then was removed and dissected to obtain the left ventricle plus interventricular septum. All subsequent procedures were carried out at 2−4 °C.

Washed membranes were prepared from the pooled ventricles from 15−25 animals. The tissue was homogenized by means of a Brinkman Polytron (setting 7, 20 s) followed by several passes in a Potter-Elvehjem tissue blender with a Teflon pestle. The homogenate was centrifuged for 30 min at 113000*g*, and the pellets were stored at −75 °C. Membranes were washed by resuspending thawed pellets in buffer (5.0 mM HEPES, pH 8.0) containing EDTA (1.0 mM) and bacitracin (200 μg/mL). The pellets were disrupted by one burst of the Polytron (setting 7, 10 s), and the homogenate was centrifuged for 30 min at 72000*g*. This procedure was carried out a total of three times. The membranes then were resuspended a fourth time, and the homogenate was divided into aliquots containing sufficient material for one experiment; pellets obtained following centrifugation for 30 min at 131000*g* were stored at −75 °C.

The washing procedure described above was directed toward endogenous ligands and their misleading effects on the binding properties of G protein-linked receptors [*e.g.*, Lad *et al.* (1980)]. EDTA was included to facilitate the removal of GDP from receptor-linked G proteins (Gilman, 1987), but membranes washed with EDTA alone were found to exhibit a time-dependent loss of specific binding when incubated with *N*-[^{3}H]methylscopolamine under the conditions of the binding assay. Bacitracin and several protease inhibitors were tested for their protective effect, and the combination of EDTA and bacitracin in the washing buffer was found to yield a preparation in which binding is stable for at least 4 h at 30 °C.[2] Membranes prepared in this manner exhibit the muscarinic binding and regulatory properties characteristic of cardiac muscarinic receptors. The present results and those described previously suggest that the preparations contained little or no endogenous GDP (Chidiac *et al.*, 1991; Chidiac and Wells, 1992).

Binding Assays. A Potter-Elvehjem tissue blender was used to resuspend washed membranes in buffer A [50 mM HEPES (Calbiochem), 1.0 mM $MgCl_2$, pH 7.45, 6−8 mg of protein per mL] or buffer B [10 mM HEPES (Boehringer), 5.0 mM $MgCl_2$, 100 mM NaCl, 1.0 mM EGTA, 1.0 mM dithiothreitol, 0.1 mM phenylmethanesulfonyl fluoride, pH 7.40], and the suspension was passed through three layers of cheesecloth. Protein was measured according to the Lowry procedure, with bovine serum albumin taken as the standard. As described below, the binding of *N*-[^{3}H]-methylscopolamine to muscarinic receptors is more informative when measured in buffer A: in particular, the radioligand is sensitive to GMP-PNP, as noted previously (Hulme *et al.*, 1981), and there was better definition of the multiple states recognized by agonists. As described in the accompanying paper (Green *et al.*, 1997), assays in buffer B permit a comparison between the binding properties of the receptor and those of receptor-linked G proteins labeled by [^{35}S]-GTPγS.

The resuspended material was diluted with the same buffer to yield a final protein concentration of 0.67 g/L (buffer A) or 0.5 g/L (buffer B). Aliquots of the suspension (490 μL) then were added to polypropylene microcentrifuge tubes containing the radioligand (5 μL) and any other ligands (5 μL) dissolved in deionized water at 100 times the final concentration. Samples containing [^{3}H]quinuclidinylbenzilate were incubated for 2 h; those containing *N*-[^{3}H]-methylscopolamine were incubated for either 45 min (buffer A) or 2.5 h (buffer B). Incubations were carried out at 30 °C, and bound radioligand was separated by microcentrifugation. Subsequent procedures were as described previously (Wong *et al.*, 1986). All assays were carried out in quadruplicate, and each sample was counted twice; the eight values then were averaged to obtain the mean and standard

[2] M. A. Green, A. Vigor, and J. W. Wells, unpublished observations.

Scheme 1

$$PR_j \underset{[P]/K_{Pj}}{\rightleftharpoons} R_j \overset{[A]/K_{Aj}}{\rightleftharpoons} AR_j$$

error used in subsequent analyses. Standard errors from assays with *N*-[^{3}H]methylscopolamine typically were about 0.5% of the mean and rarely exceeded 1%.

Reaction with Propylbenzilylcholine Mustard. Solutions of the mustard (10 μM) in buffer (10 mM HEPES, 1.0 mM $MgCl_2$, pH 7.45) were kept at room temperature for 1 h to obtain the aziridinium ion. Aliquots then were added to washed membranes previously resuspended in ice-cold buffer (10 mM HEPES, 1.0 mM $MgCl_2$, pH 7.45, 1.2−1.4 mg of protein per mL) by means of the Polytron (setting 7, 10 s) and preincubated for 5 min at 30 °C. The reaction mixture was incubated for 15 min at 30 °C. The homogenate then was centrifuged for 20 min at 3 °C and 85000*g*, and the membranes were washed as described above. To obtain tissue for control experiments, the mustard was omitted from an otherwise identical procedure.

Analysis of Data. All data were analyzed with total binding taken as the dependent variable (B_{obsd}, dpm/mL). Any subsequent manipulations were for the purpose of presentation only and did not alter the relationship between the data and the fitted curve.

Data were described empirically in terms of the Hill equation to obtain estimates of the asymptotic levels of binding, the Hill coefficient (n_H), and the concentration of ligand required for a half-maximal signal (EC_{50}). Fits to data obtained at graded concentrations of *N*-[^{3}H]methylscopolamine or [^{3}H]quinuclidinylbenzilate included an implicit correction for depletion of the radioligand [*i.e.*, eq 204 in Wells (1992)]; otherwise, it was assumed that the free and total concentrations were equal for all ligands.

Empirical analyses also were carried out according to eqs 1 and 2, in which the parameters $B_{[A]=0}$ and $B_{[A]\to\infty}$ represent the asymptotic levels of binding with respect to the total concentration of the unlabeled ligand ($[A]_t$). The parameters K_j (eq 1) and K_{1j} (eq 2) represent the value of $[A]_t$ required for a half-maximal effect at the fraction F'_j or F'_{1j} of the total potential change in B_{obsd} ($j = 1, 2, ..., n$). Equation 2 is an extension of eq 1 in which an additional process, characterized by K_2 and n_H, affects B_{obsd} in the opposite sense [*cf.* eq 223 in Wells (1992)]. The parameters *a* and *b* define the intrinsic amplitude of the peak or trough, and the present data were described in terms of *b*.

$$B_{obsd} = (B_{[A]=0} - B_{[A]\to\infty}) \sum_{j=1}^{n} \frac{F'_j K_j}{K_j + [A]_t} + B_{[A]\to\infty} \quad (1)$$

$$B_{obsd} = B_{[A]=0} + a\left(\sum_{j=1}^{n} \frac{F'_{1j}[A]_t}{K_{1j} + [A]_t}\right)\left(\frac{K_2^{n_H} + b[A]_t^{n_H}}{K_2^{n_H} + [A]_t^{n_H}}\right) \quad (2)$$

$$\text{where} \qquad ab = B_{[A]\to\infty} - B_{[A]=0}$$

Mechanistic descriptions of the data were based on two possibilities that predict Hill coefficients <1: intrinsic heterogeneity (Scheme 1) and cooperativity (Scheme 2). A third possibility, heterogeneity induced through an interaction with the G protein, is considered in the accompanying paper (Green *et al.*, 1997). Estimates of total binding were fitted

Scheme 2

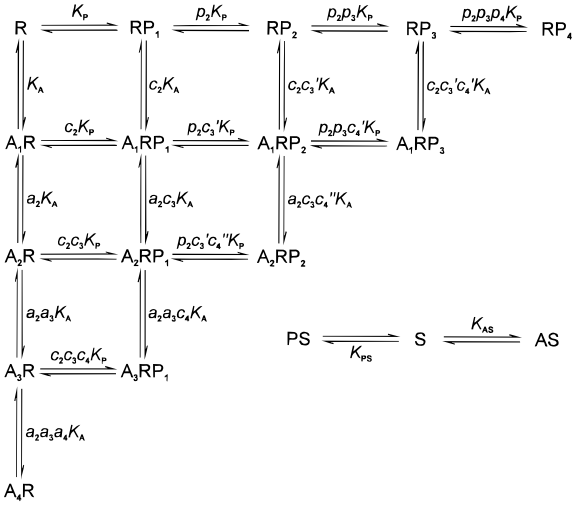

by eq 3, in which $[P]_b$ represents the specific binding of the radioligand at a total concentration $[P]_t$; SA is the specific radioactivity (Ci/mmol), and NS is the fraction of unbound radioligand that appears as nonspecific binding.

$$B_{obsd} = \{[P]_b + (NS)([P]_t - [P]_b)\}(SA)(2.22 \times 10^{12}) \quad (3)$$

Scheme 1 represents a multisite model in which the radioligand (P) and an unlabeled ligand (A) compete for a mixture of distinct and mutually independent sites (R_j, $j = 1, 2, ..., n$). Sites of type *j* bind P and A with the equilibrium dissociation constants K_{Pj} and K_{Aj}, respectively, and constitute the fraction F_j of all sites (*i.e.*, $F_j = [R_j]_t/[R]_t$, where $[R_j]_t = [R_j] + [AR_j] + [PR_j]$, and $[R]_t = \sum_{j=1}^{n}[R_j]_t$). Total specific binding of the probe was calculated according to eq 4, and the required values of $[PR_j]$ were obtained as described below.

$$[P]_b = \sum_{j=1}^{n} [PR_j] \quad (4)$$

Cooperativity was modeled according to Scheme 2, in which R and S represent tetravalent ($n = 4$) and monovalent receptors, respectively. Bivalent ($n = 2$) and trivalent ($n = 3$) receptors are described by truncated forms of R. The multivalent species is likely to be oligomeric, and it is assumed that the quaternary structure remains formally intact under the conditions of the binding assays; that is, there is no exchange of individual subunits within the system. The model therefore can accommodate processes in which dissociated monomers regroup without exchanging partners. There is no relationship between R and S, which are defined as mutually independent and noninterconverting.

Asymmetry cannot be detected with the present data, and all sites of the vacant oligomer (R) are assumed to bind the radioligand (P) or the unlabeled ligand (A) with the microscopic dissociation constant K_P or K_A (*e.g.*, $K_P = [P][R]/[PR]$). The parameters p_j and a_j represent the cooperativity factors for binding of the *j*th equivalent of P or A to form RP_j or A_jR, respectively ($j \geq 2$) (*e.g.*, $[RP_{j-1}][P]/[RP_j] = \Pi_{i=2}^{j} p_i K_P$); the parameters c_j, c'_j, and c''_j represent cooperativity factors in the formation of mixed complexes,

as shown in Scheme 2. The dissociation constants for binding to the monovalent species S are K_{PS} and K_{AS}.

Total specific binding was calculated according to eq 5.1, 5.2, or 5.3 for the divalent, trivalent, or tetravalent forms of R, respectively. Coefficients >1 represent the degree of occupancy by P, since R is defined as multivalent, times the number of possible combinations involving two ligands and n sites. Since stoichiometrically equivalent states are indistinguishable with the present data, the microscopic dissociation constant was taken as the same for all vacant sites on partially liganded R (*e.g.*, [P][POOA]/[PPOA] = [P][POOA]/[POPA], where "O" represents a vacant site on tetravalent R). The triliganded species A_2RP_1 and A_1RP_2 also were taken as identical (*i.e.*, $c_3 = c'_3$), as were the tetraliganded species A_3RP_1, A_2RP_2, and A_1RP_3 (*i.e.*, $c_4 = c'_4 = c''_4$). These latter forms are not necessarily indistinguishable in binding studies, but the additional parameters were found to be without effect on the sum of squares.

$$[P]_b = [PS] + 2[RP] + 2[RP_2] + 2[ARP] \quad (5.1)$$

$$[P]_b = [PS] + 3[RP] + 6[RP_2] + 3[RP_3] + 6[ARP] + 3[A_2RP] + 6[ARP_2] \quad (5.2)$$

$$[P]_b = [PS] + 4[RP] + 12[RP_2] + 12[RP_3] + 4[RP_4] + 12[ARP] + 12[A_2RP] + 24[ARP_2] + 12[A_2RP_2] + 4[A_3RP] + 12[ARP_3] \quad (5.3)$$

The value of $[P]_b$ in eqs 4−5.3 was calculated from the expansions in terms of the total concentrations of R and S ($[R]_t$, $[S]_t$) and the free concentrations of both ligands ([A], [P]).[3] The relevant expressions were used directly to obtain the simulations in Figures 7 (eq 5.1) and 8 (eq 5.3). In all analyses of experimental data, which generally included instances of depletion, the values of [A] and [P] used to compute $[P]_b$ were obtained by solving a set of implicit equations derived from the equations of state for all reactants. Solutions were obtained according to the Newton−Raphson procedure. Further details regarding the formulation of Schemes 1 and 2 have been described elsewhere (Wells, 1992; Green *et al.*, 1997). Except for simulations (*i.e.*, Figures 7−9), values plotted on the abscissa denote total concentration in all figures.

Data from replicated experiments have been presented with reference to a single fitted curve in figures that illustrate the results of simultaneous analyses. To obtain the values plotted on the ordinate, estimates of B_{obsd} were adjusted according to

$$B'_{obsd} = B_{obsd}\frac{f(\bar{\mathbf{x}}_i,\bar{\mathbf{a}})}{f(\mathbf{x}_i,\mathbf{a})} \quad (6)$$

The function f represents the fitted model. The vectors $\mathbf{x}_i$ and $\mathbf{a}$ represent the independent variables at point i and the fitted parameters for the set of data under consideration; $\bar{\mathbf{x}}_i$ and $\bar{\mathbf{a}}$ are the corresponding vectors in which values that differ from experiment to experiment have been replaced by the means for all experiments included in the analysis. Individual values of B'_{obsd} at the same $\mathbf{x}_i$ were averaged to obtain the mean and standard error plotted in the figure.

Statistical Procedures. All parameters were estimated by nonlinear regression, and values at successive iterations of the fitting procedure were adjusted according to the algorithm of Marquardt (1963). Most analyses involved multiple sets of data, and specific details regarding the assignment of shared parameters are described where appropriate. Values of $[R]_t$ or $[R]_t + [S]_t$ were assigned separately to data from separate experiments and, in most cases, to data acquired in the absence and presence of GMP-PNP within the same experiment. Values of NS were separate for data from different experiments but were common to all data from the same experiment.

Weighting of the data, tests for significance, and other statistical procedures were performed as described elsewhere (Wong *et al.*, 1986; Wells, 1992; Chidiac and Wells, 1992). Weighted residuals were of comparable magnitude within single sets of data, and multiple sets of data generally made comparable contributions to the total sum of squares from simultaneous analyses; accordingly, neither the total sum of squares nor the correlation of neighboring residuals was dominated by the data from one experiment or group of experiments. Mean values calculated from two or more individual estimates of a parameter or other quantity are presented together with the standard error. For parametric values derived from a single analysis of one or more sets of data, the errors were estimated from the diagonal elements of the covariance matrix; such values reflect the range within which the weighted sum of squares is essentially the same.

RESULTS

Binding in Terms of Empirical Models and Scheme 1

Binding of Antagonists to Native Membranes. Specific binding at graded concentrations of [^{3}H]quinuclidinylbenzilate in buffer A revealed Hill coefficients indistinguishable from 1. The corresponding capacity was 141−177 pmol/g of protein in membranes from three batches of hamsters. The apparent capacity for *N*-[^{3}H]methylscopolamine was 102−117 pmol/g of protein, which represents 66%, 70%, or 75% of the capacity for [^{3}H]quinuclidinylbenzilate in membranes from the same batch of tissue. Assays in buffer B similarly revealed more sites for [^{3}H]quinuclidinylbenzilate than for *N*-[^{3}H]methylscopolamine, but the difference in capacity is not well-defined by the data. Binding was comparatively weak, as described below, and the nonspecific contribution was high at near-saturating concentrations of either radioligand.

[3] The binding function in each case was of the form $[P]_b = f([A], [P], \mathbf{a})$, where $\mathbf{a}$ represents the vector of all parameters and constants. Those entered explicitly into the calculation are as follows: eq 4, K_{Aj}, K_{Pj}, F_j, and $[R]_t$; eqs 5.1−5.3, K_A, K_P, a_j, p_j, c_j, K_{AS}, K_{PS}, $[R]_t + [S]_t$, and $[R]_t/([R]_t + [S]_t)$. Microscopic dissociation constants for the binding of A or P to the cooperative form of the receptor in Scheme 2 were computed as required (*e.g.*, $\Pi_{i=2}^{j} a_i K_A$ for the reaction $[A] + [A_{j-1}R] \rightleftharpoons [A_jR]$, $\Pi_{i=2}^{j-1} a_i c_i K_A$ for the reaction $[A] + [A_{j-1}RP] \rightleftharpoons [A_jRP]$, etc.). The values of $[R_j]_t$ in Scheme 1 were computed from F_j and $[R]_t$. The values of $[R]_t$ and $[S]_t$ in Scheme 2 were computed from $[R]_t + [S]_t$ and $[R]_t/([R]_t + [S]_t)$, where the latter represents the fraction of all receptors corresponding to the multivalent form (*i.e.*, F_R). Since the stoichiometry of binding is n:1 for R and 1:1 for S, the fraction of binding sites contributed by R is $nF_R/[(n-1)F_R + 1]$; similarly, the fraction of sites contributed by S is $(1 - F_R)/[(n-1)F_R + 1]$. The model is formally equivalent to Scheme 2 when the noncooperative form of the receptor is defined as multivalent but functionally symmetrical. If the stoichiometry of binding is the same for both forms, the quantity $[R]_t/([R]_t + [S]_t)$ is equal to the fraction of sites contributed by R.

Table 1: Direct and Inferred Binding of *N*-[^{3}H]Methylscopolamine in Terms of Scheme 1[a]

conditions	GMP-PNP (mM)	ligand	$-\log K_{L1}$	$-\log K_{L2}$	$-\log K_{L3}$	F_1	F_2	F_3
buffer A								
A [1]	0.0	NMS	9.75 ± 0.10	10.33 ± 0.02	*b*	0.79	0.21 ± 0.11	
	0.1	NMS				0.43	0.57 ± 0.09	
B [2]	0.0	carbachol	7.81 ± 0.18	6.70 ± 0.08	5.11 ± 0.06	0.68	0.22 ± 0.02	0.11 ± 0.01
	0.0	NMS	9.59 ± 0.12	9.95 ± 0.05	10.12 ± 0.09			
C [1, 2]	0.0	carbachol	7.73 ± 0.05	6.85 ± 0.16	5.20 ± 0.12	0.68	0.22 ± 0.03	0.10 ± 0.01
	0.0	NMS	9.41 ± 0.09	10.00 ± 0.04	10.18 ± 0.03	0.24	0.66 ± 0.06	
	0.1	NMS				0.13	0.0[c]	0.87 ± 0.05
buffer B								
D [1]	0.0	NMS	9.06 ± 0.03	*d*	*d*	1.0		
	0.1	NMS						

[a] The conditions of the assays are summarized in the table, with the experimental protocol shown in brackets. In protocol 1, binding at graded concentrations of *N*-[^{3}H]methylscopolamine (L ≡ P) was measured with the radioligand alone, the radioligand plus 0.1 mM GMP-PNP, and the radioligand plus 0.01 mM unlabeled *N*-methylscopolamine (*e.g.*, Figure 4D); in protocol 2, binding at graded concentrations of carbachol (L ≡ A) was measured at two concentrations of *N*-[^{3}H]methylscopolamine (0.04 and 1.0 nM) (*e.g.*, Figure 1). Three experiments were performed under each set of conditions, and eq 4 ($n = 1$, 2, or 3) was fitted to multiple sets of data as follows. (A) Single values of K_{Pj} and separate values of F_2 were assigned to the data acquired with and without GMP-PNP in the same experiment; the fitted values from individual experiments then were averaged to obtain the means (±SEM) listed in the table. The values of $[R]_t$ are as follows: no GMP-PNP, 74−113 pmol/g of protein; with GMP-PNP, 82−114 pmol/g of protein. (B) Single values of K_{Pj}, K_{Aj}, and F_j were common to the data acquired at both concentrations of the radioligand in the same experiment; the fitted values from individual experiments then were averaged to obtain the means (±SEM) listed in the table. The range of $[R]_t$ is 95−106 pmol/g of protein. (C) Single values of K_{Pj} were common to all of the data from both protocols, and single values of K_{Aj} were common to all data from protocol 2. Single values of F_3 were common to all data acquired either with or without GMP-PNP, regardless of protocol; values of F_2 were common only to data acquired according to the same protocol (*i.e.*, protocol 1 for NMS; protocol 2 for carbachol). (D) The value of K_{P1} was obtained as described in A. The corresponding values of $[R]_t$ are as follows: no GMP-PNP, 149−167 pmol/g of protein; with GMP-PNP, 147−168 pmol/g of protein. [b] Two classes of sites are sufficient to describe the data. [c] The value is not defined by the data and was fixed at zero. [d] One class of sites is sufficient to describe the data.

GMP-PNP increased the overall affinity of *N*-[^{3}H]methylscopolamine in buffer A, as shown below in Figure 4. The mean values of log EC_{50} estimated in terms of the Hill equation are -10.10 ± 0.03 and -9.88 ± 0.02 for binding with and without the nucleotide, respectively, in three experiments; the corresponding values of the Hill coefficient are 0.91 ± 0.03 and 0.92 ± 0.05, and both are significantly less than 1 ($P < 0.00001$). Maximal specific binding varied from 74 to 94 pmol/g of protein, but the mean ratio for binding with and without GMP-PNP in the same experiment is 1.02 ± 0.05. Two classes of sites are required in terms of Scheme 1 ($P < 0.05$). There is no appreciable change in the goodness of fit if it is assumed that GMP-PNP was without effect on K_{P1} or K_{P2}, and the corresponding values of F_j point to an interconversion of sites from lower to higher affinity for the antagonist (Table 1A).

While two classes of sites can be resolved by graded concentrations of the radioligand, data presented below indicate that agonists differentiate among at least three classes. The affinity of *N*-[^{3}H]methylscopolamine for the sites of each class discerned by agonists can be estimated from the inhibitory behavior of carbachol at two concentrations of the radioligand. Data from one experiment at low ionic strength are illustrated in Figure 1, where the lines represent the best fit of Scheme 1 (eq 4). The mean estimates of affinity from three such experiments indicate that carbachol and *N*-[^{3}H]methylscopolamine are opposite in their preference for the three classes of sites (Table 1B).

Data acquired at graded concentrations of *N*-[^{3}H]methylscopolamine and carbachol were pooled to obtain the parametric values listed in Table 1C. Independent analyses imply that the radioligand is slightly more potent alone (Table 1A, log $EC_{50} = -9.86$[4]) than in competition with carbachol (Table 1B, log $EC_{50} = -9.72$[4]). In the combined analysis, this anomaly leads to small but significant discrepancies in

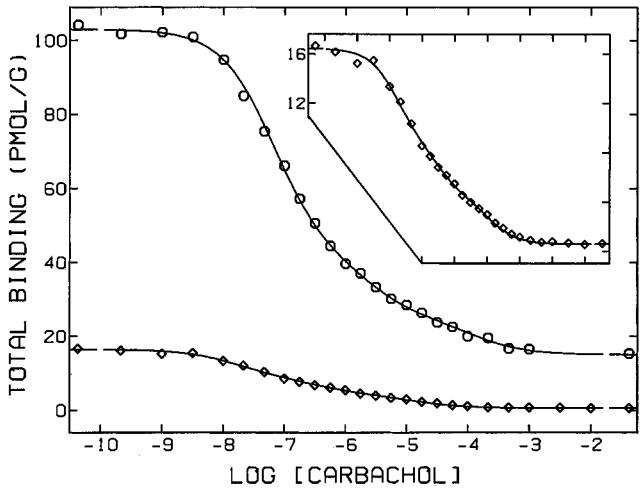

FIGURE 1: Inhibition of *N*-[^{3}H]methylscopolamine by carbachol at two concentrations of the radioligand. Total binding was measured following equilibration of the membranes (buffer A) with [^{3}H]NMS (○, 1.03 nM; ◇, 0.040 nM) and carbachol at the concentrations shown on the abscissa. The points are from a single experiment, and the lines represent the best fit of eqs 3 and 4 ($n = 3$) to the two sets of data taken together. All parameters were common to both sets of data, and the fitted values are as follows: log $K_{A1} = -7.90 \pm 0.04$, log $K_{A2} = -6.64 \pm 0.13$, log $K_{A3} = -5.13 \pm 0.11$, log $K_{P1} = -9.63 \pm 0.04$, log $K_{P2} = -10.00 \pm 0.07$, log $K_{P3} = -10.18 \pm 0.05$, $F_2 = 0.17 \pm 0.01$, $F_3 = 0.099 \pm 0.009$, $[R]_t = 70.8 \pm 0.8$ pM, and NS $= 0.0097 \pm 0.0001$. Points shown at the lower and upper ends of the abscissa indicate binding in the absence of carbachol and in the presence of 0.01 mM unlabeled NMS, respectively. The results of three such experiments were averaged to obtain the means listed in Table 1B. The data acquired at 0.040 nM [^{3}H]NMS are plotted on an expanded scale in the inset.

Table 2: Binding of *N*-[^{3}H]Methylscopolamine: Affinity and Relative Capacity for Agonists in Terms of Scheme 1[a]

agonist	buffer and membranes	GMP-PNP (mM)	$-\log K_{A1}$	$-\log K_{A2}$	$-\log K_{A3}$	F_1	F_2	F_3
carbachol	A, native	0.0	7.77 ± 0.07	6.78 ± 0.08	5.08 ± 0.08	0.69	0.20 ± 0.03	0.11 ± 0.01
		0.1		5.73 ± 0.06		0.11	0.50 ± 0.05	0.39 ± 0.05
arecoline	A, native	0.0	7.87 ± 0.11	7.09 ± 0.36	5.19 ± 0.12	0.56	0.31 ± 0.11	0.13 ± 0.02
		0.1		5.85 ± 0.16		0.09	0.51 ± 0.11	0.40 ± 0.12
methacholine	A, native	0.0	7.83 ± 0.09	6.83 ± 0.17	5.37 ± 0.06	0.74	0.16 ± 0.01	0.10 ± 0.01
		0.1		6.06 ± 0.04		0.08	0.51 ± 0.03	0.41 ± 0.02
carbachol	A, alkylated	0.0	7.73 ± 0.07	6.73 ± 0.12	5.52 ± 0.06	0.75	0.10 ± 0.06[b]	0.15 ± 0.03
		0.1				0.07[c]	0.29 ± 0.04	0.64 ± 0.04
carbachol	B, native	0.0	6.94 ± 0.28	5.21 ± 0.26	3.68 ± 0.27	0.42	0.47 ± 0.05	0.12 ± 0.04
		0.1		4.74 ± 0.17		0.07	0.49 ± 0.18	0.43 ± 0.18

[a] Binding to native and alkylated membranes was measured in the absence and presence of GMP-PNP as described in the text and in the legends to Figures 4A−C, 5A, and 6A; the alkylated preparation was obtained by pretreatment with propylbenzilylcholine mustard. Equation 4 ($n = 3$) was fitted to the data from each of three experiments taken separately. The dissociation constant of the radioligand for each class of sites was fixed as follows: buffer A, $\log K_{P1} = -9.414$, $\log K_{P2} = -9.999$, $\log K_{P3} = -10.183$ (Table 1C); buffer B, $\log K_{P1} = -9.062$ (Table 1D). Data acquired with and without the nucleotide in the same experiment shared single values of K_{A1} and K_{A3} (native membranes) or of K_{A1}, K_{A2}, and K_{A3} (alkylated membranes); other parameters were assigned separately. Estimates of K_{Aj} and F_j from individual experiments were averaged to obtain the means (±SEM) listed in the table. [b] The value of F_2 is indistinguishable from zero for one set of data acquired in the absence of GMP-PNP. [c] The value of F_1 is indistinguishable from zero for two sets of data acquired in the presence of GMP-PNP.

F_j for binding in the absence of GMP-PNP (Table 1C).

Binding of *N*-[^{3}H]methylscopolamine was unaffected by GMP-PNP at higher ionic strength (buffer B), as described previously for cardiac membranes suspended in a modified Krebs−Henseleit solution (Wong *et al.*, 1986). The mean values of log EC_{50} are -9.09 ± 0.03 and -9.05 ± 0.05 for binding with and without the nucleotide, respectively, and the corresponding values of n_H are 1.02 ± 0.01 and 0.99 ± 0.01 ($N = 3$). The mean ratio of maximal specific binding with and without the nucleotide is 0.98 ± 0.01. One class of sites is sufficient in terms of Scheme 1, and GMP-PNP was without significant effect on the value of K_{P1} (Table 1D).

Apparent Distribution of Sites and Affinity for Agonists in Native Membranes. At low ionic strength, the agonists carbachol, arecoline, and methacholine recognized three classes of sites either with or without GMP-PNP. Essentially the same pattern emerged at high ionic strength, at least for carbachol, although the sites of highest affinity were almost undetectable in the presence of GMP-PNP. There is little or no change in the global sum of squares for any agonist if GMP-PNP is assumed not to affect K_{A1} and K_{A3} ($P > 0.03$), and the parametric values from those analyses are listed in Table 2; in contrast, there is a significant increase if the same constraint is placed on K_{A1} and K_{A2} ($P < 0.02$) or on K_{A2} and K_{A3} ($P < 0.03$). GMP-PNP therefore caused a 3.0−17-fold increase in K_{A2} with no appreciable change in K_{A1} or K_{A3}. The corresponding values of F_j indicate that sites were lost from the state of highest affinity and gained in the two states of lower affinity (Table 2). The net gain in each of the latter was almost equal in buffer A, while the state of lowest affinity was favored in buffer B. The fitted curves from Scheme 1 are virtually indistinguishable from those illustrated in Figures 4 and 6, which represent the best fits of Scheme 2 to the same data (please see below).

Sites of intermediate and low affinity in the absence of GMP-PNP appear not to reflect residual levels of endogenous ligands such as GDP. Membranes washed with bacitracin and 10 mM EDTA revealed three classes of sites for carbachol at low ionic strength, and the values of F_j agree well with those listed in Table 2 (buffer A) (*i.e.*, $F_1 = 0.69$, $F_2 = 0.12 \pm 0.03$, $F_3 = 0.19 \pm 0.03$). Three classes of sites and comparable values of F_j also were obtained when membranes prepared as described under Materials and Methods were assayed in buffer A containing 1.0 mM EDTA rather than magnesium (*i.e.*, $F_1 = 0.51 \pm 0.04$, $F_2 = 0.34 \pm 0.03$, $F_3 = 0.15$).

Sites of high and intermediate affinity that coexist with GMP-PNP represent a limiting state of the system and not a subsaturating concentration of the nucleotide. As illustrated in Figure 2A, the inhibitory effect of 0.56 μM carbachol at low ionic strength was reversed only partially at high concentrations of GMP-PNP (*i.e.*, >10 μM). Had all of the sites been in the state of low affinity for the agonist, specific binding of the radioligand would have been inhibited by <1% under those conditions (*i.e.*, $\log K_{P3} = -10.18$, Table 1C; $\log K_{A3} = -5.08$, Table 2). The data reveal a dispersion of affinities for GMP-PNP ($n_H = 0.77 \pm 0.05$), which requires two classes of sites in terms of eq 1.

A similar pattern was observed with GMP-PNP, GTPγS, and GDP at high ionic strength (Figure 2B). The inhibitory effect of 10 μM carbachol was reversed only partially at saturating concentrations of nucleotide, and the dose dependence points to multiple forms or states of the G protein. GMP-PNP and GTPγS both revealed two classes of sites, and the effect was consistently to reduce binding of the agonist. GDP revealed at least three classes, and binding to those of highest affinity promoted binding of the agonist; binding to those of lower affinity reduced binding of the agonist, and the dose dependence exhibits a Hill coefficient of 1.4 ± 0.1.

Apparent Affinity and Distribution of Sites following Partial Alkylation. Irreversible blockade by propylbenzilylcholine mustard exhibited the dose dependence illustrated in Figure 3. The Hill coefficient is indistinguishable from 1, and sufficient concentrations of the mustard resulted in complete blockade. On the basis of the value of 1.7 nM obtained for K_1 (eq 1, $n = 1$), a concentration of 5.6 nM

[4] Values of EC_{50} were calculated from the fitted estimates of K_{Lj} and F_j listed for *N*-methylscopolamine in Table 1.

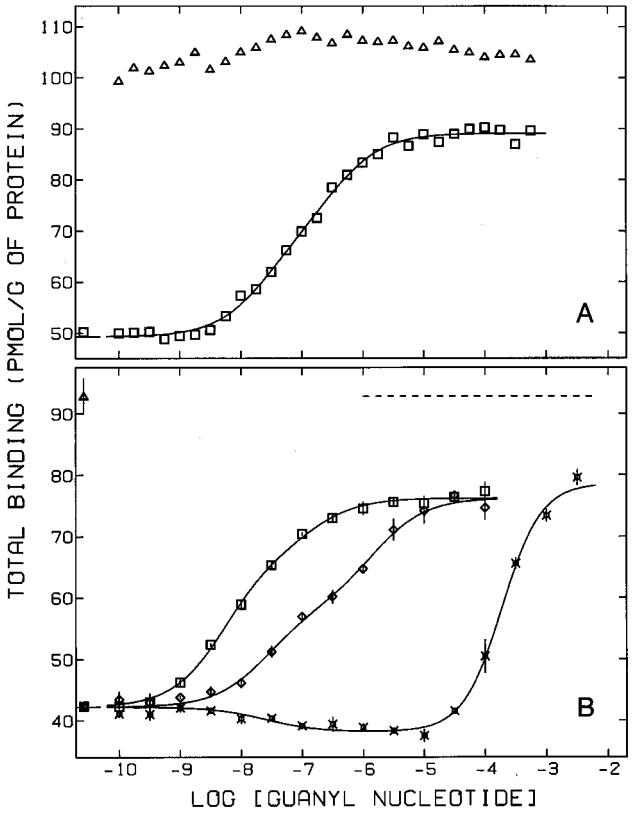

FIGURE 2: Effect of guanyl nucleotides on the inhibition of *N*-[^{3}H]-methylscopolamine by carbachol. Total binding was measured following equilibration of the membranes in buffer A (A) or buffer B (B) with [^{3}H]NMS (A, 1.00 nM; B, 1.01−1.09 nM), carbachol (A, 0.56 μM; B, 10 μM) and one of GMP-PNP (□), GTPγS (◊), or GDP (⊗) at the concentrations shown on the abscissa. Total binding in the absence of carbachol is denoted by triangles (Δ) and by the dashed line in panel B. The line in panel A represents the best fit of eq 1 ($n = 2$), and the fitted parametric values are as follows: log $K_1 = -7.61 \pm 0.15$, log $K_2 = -6.47 \pm 0.18$, $F'_2 = 0.50 \pm 0.12$, $B_{[A]=0} = 49.3 \pm 0.4$ pmol/g of protein, and $B_{[A]\to\infty} = 89.1 \pm 0.4$ pmol/g of protein. The lines in panel B represent the best fit of eq 2 to a total of nine sets of data from three experiments, where each experiment included one curve per nucleotide. Single values of K_{1j}, F'_{1j}, K_2, n_H, and b were common to all data acquired with the same nucleotide, and the fitted estimates are as follows: GMP-PNP ($n = 2$, $b = 1$), log $K_{11} = -8.28 \pm 0.12$, log $K_{12} = -6.87 \pm 0.41$, $F'_{12} = 0.26 \pm 0.11$; GTPγS ($n = 2$, $b = 1$), log $K_{11} = -7.57 \pm 0.14$, log $K_{12} = -5.84 \pm 0.17$, $F'_{12} = 0.52 \pm 0.06$; GDP ($n = 1$), log $K_{11} = -7.61 \pm 0.29$, log $K_2 = -3.73 \pm 0.04$, $n_H = 1.4 \pm 0.1$, $b = -8.9 \pm 1.2$. A single value of $B_{[A]=0}$ was common to all data from the same experiment, and the mean of the three values is 42 ± 3 pmol/g of protein. A separate value of $B_{[A]\to\infty}$ was assigned to each set of data, and the mean for each nucleotide is as follows (pmol/g of protein): GMP-PNP, 76 ± 2; GTPγS, 76 ± 2; GDP, 79 ± 2. Nonspecific binding was 14 ± 1 pmol/g of protein. Values plotted on the ordinate were obtained according to eq 6. Points shown at the lower end of the abscissa represent binding in the absence of nucleotide.

was selected for the reaction between the reagent and a quantity of membranes sufficient for subsequent characterization of the binding properties. The expected level of alkylation is about 77%.

The binding of *N*-[^{3}H]methylscopolamine to unreacted sites in the alkylated membranes revealed a dispersion of affinities and remained sensitive to GMP-PNP, although the effects are comparatively small. The sum of squares is significantly lower with two classes of sites rather than one, regardless of whether separate or common values of K_{Pj} are assigned to data acquired with and without the nucleotide

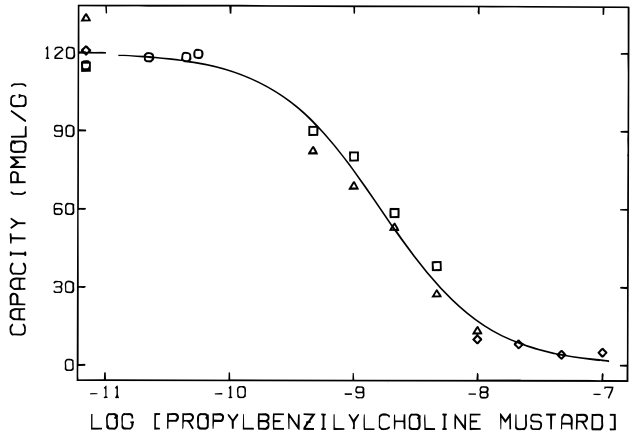

FIGURE 3: Irreversible blockade by propylbenzilylcholine mustard. Aliquots from homogenates of washed membranes were reacted with the mustard at the concentrations plotted on the abscissa; values plotted at the lower limit represent samples from which the mustard was omitted. Different symbols represent different experiments. Levels of binding in the treated membranes were measured at a single concentration of [^{3}H]NMS (0.92−1.05 nM) alone and in the presence of 0.01 mM unlabeled NMS. The corresponding estimates of capacity (*i.e.*, $[R]_t$) were computed according to eq 4 ($n = 3$), with K_{Pj} and F_j taken as the values listed for the antagonist in Table 1C. Estimates of $[R]_t$ from the four experiments then were analyzed simultaneously in terms of eq 1 ($n = 1$) with $B_{[A]\to\infty}$ fixed at zero; one value of K_1 was common to all of the data, and separate values of $B_{[A]=0}$ were assigned to the data from individual experiments. The sum of squares was not reduced significantly if $B_{[A]\to\infty}$ was taken as a variable during the fitting procedure ($P > 0.1$). To obtain the values plotted on the ordinate, individual estimates of $[R]_t$ were normalized to the appropriate value of $B_{[A]=0}$ taken as the mean from the four experiments. The line illustrates the best fit, and the fitted value of log K_1 is -8.78 ± 0.05.

($P < 0.005$). GMP-PNP favored the state of higher affinity, as in native membranes, and the fit is compromised with single values for all three of K_{P1}, K_{P2}, and F_2 ($P = 0.0064$). The values of K_{Pj} and F_2 are not well-defined with alkylated membranes, owing largely to the comparatively small signal, but there is little change in the global sum of squares when pooled data from treated and control preparations share common values of all parameters except $[R]_t$ and NS ($P = 0.031$); the fitted curves are in excellent agreement with the data, and the parametric values compare favorably with those listed in Table 1A.[5] Treatment with the mustard reduced total capacity for the radioligand by 79−81%, in good agreement with the loss predicted on the basis of the data illustrated in Figure 3.

Binding of carbachol to the alkylated membranes revealed three classes of sites at low ionic strength in the absence of

[5] A suspension of washed tissue was divided into two portions, one of which was reacted with 5.6 nM propylbenzilylcholine mustard and processed as described under Materials and Methods. The other was carried through a parallel procedure from which the mustard was omitted. Binding of *N*-[^{3}H]methylscopolamine to the control and alkylated membranes was measured with and without GMP-PNP (*cf.* Figure 4D), and the data were analyzed in terms of Scheme 1 (eqs 3 and 4). Single values of K_{P1} and K_{P2} were common to all of the data, and separate values of F_2 were assigned to data acquired either with or without the nucleotide. The fitted estimates of all parameters are as follows: log $K_{P1} = -9.91 \pm 0.11$, log $K_{P2} = -10.44 \pm 0.26$, $F_2 = 0.13 \pm 0.21$ (no GMP-PNP) and 0.32 ± 0.27 (with GMP-PNP), $[R]_t$ (native membranes) $= 89 \pm 1$ pmol/g of protein (no GMP-PNP) and 92 ± 1 pmol/g (with GMP-PNP), $[R]_t$ (alkylated membranes) $= 16.8 \pm 0.5$ pmol/g (no GMP-PNP) and 19.4 ± 0.4 pmol/g (with GMP-PNP), and NS $= 0.0093 \pm 0.0001$ (native membranes) and 0.0091 ± 0.0001 (alkylated membranes).

GMP-PNP. Two classes of sites are sufficient overall in the presence of GMP-PNP, although one experiment suggested a third ($P = 0.046$). There is no increase in the sum of squares with common values of all K_{Aj} for data acquired with and without the nucleotide in each experiment ($P = 0.47$), and the mean parametric values are listed in Table 2. Partial inactivation therefore eliminated the nucleotide-dependent increase in K_{A2} observed with native membranes. Changes in F_j indicate that alkylation almost eliminated the sites of medium affinity in the absence of GMP-PNP, while the sites of high affinity remained at native levels in relative terms. Most of the latter were sensitive to the nucleotide, and the interconversion was largely to the state of lowest affinity. The fitted curves from Scheme 1 are virtually indistinguishable from those illustrated in Figure 5, which represent the best fit of Scheme 2 to the same data (please see below).

Binding in Terms of Scheme 2

In the absence of evidence to the contrary, a dispersion of affinities can be described exclusively in terms of cooperative effects. If the sites of high affinity represent the vacant receptor, those of lower affinity reflect the changes induced by successive equivalents of bound ligand. Partial inactivation is expected to reduce the potential for interactions among functionally viable sites and thereby to reduce the likelihood of cooperative effects if the unreacted sites cannot regroup. As it happened, however, muscarinic receptors that eluded the mustard retained the sites of lowest affinity for carbachol in the absence of GMP-PNP (Table 2). Those sites therefore appear to be intrinsically of low affinity, and they are accounted for by the monovalent, noncooperative form of the receptor shown as S in Scheme 2.

All of the analyses included data acquired with and without GMP-PNP at graded concentrations of *N*-[^{3}H]methylscopolamine on the one hand and one or more agonists on the other. Since the two forms of the receptor are defined as noninterconverting, the quantity $[R]_t/([R]_t + [S]_t)$ was assumed to be the same for all ligands and unaffected by the nucleotide. This constraint had little or no effect on the goodness of fit, even in the comparatively simple case of a divalent plus a monovalent receptor. The affinity of the noncooperative form of the receptor generally was unaffected by GMP-PNP, and single values of K_{PS} and K_{AS} were assigned accordingly in most analyses.

If there are two competing ligands, the n interacting sites of Scheme 2 are associated with $n(n + 3)/2$ parameters exclusive of $[R]_t$. Parameters unique to the radioligand (*i.e.*, K_P, p_j) could be estimated for all values of n, at least to within a first approximation. In contrast, those unique to the unlabeled ligand (*i.e.*, K_A, a_j) or dependent upon both ligands (*i.e.*, c_j) tend to be correlated and undefined. Such parameters were mapped as required and fixed appropriately to achieve convergence to the minimum sum of squares. Despite this uncertainty, the inhibitory behavior of agonists determines or influences capacity as represented by the relative numbers of R and S [*i.e.*, $[R]_t/([R]_t + [S]_t)$] and the total number of receptors (*i.e.*, $[R]_t + [S]_t$).

Native Membranes at Low Ionic Strength. The results summarized in Table 3 are from seven analyses in which the cooperative form of the receptor was taken as divalent, trivalent, or tetravalent. Each analysis included all of the data represented in Figure 4, where the lines illustrate the fit obtained with tetravalent R as described below. Scheme 2 can account superficially for three classes of sites when R is only divalent [*e.g.*, Mattera *et al.* (1985)], and the fitted curves obtained with di- and trivalent R are almost indistinguishable from those shown in the figure.

The parametric values listed in Table 3A are obtained when *N*-methylscopolamine is assumed to exhibit little or no homotropic cooperativity in the absence of GMP-PNP. Since the fitted value of p_j is near 1 for each successive equivalent of the radioligand, all forms of the receptor were saturated or nearly so at the highest concentrations used in the assays. Under these conditions, GMP-PNP is found to increase the inferred capacity of the membranes for *N*-[^{3}H]-methylscopolamine (*i.e.*, $[R]_t + [S]_t$): the change is 1.8-fold when R is assumed to be divalent and decreases to 1.3-fold when R is tetravalent (Table 3A). A nucleotide-dependent increase in capacity is inconsistent with Scheme 2, which represents all receptors physically accessible to *N*-[^{3}H]-methylscopolamine; accordingly, the cooperative form of the receptor must be at least tetravalent if the observed capacity for the radioligand indeed corresponds to the capacity as defined by the model.

The anomalous effect on $[R]_t + [S]_t$ is linked to the value of p_n, which is near 1 in the absence of nucleotide but at least 100 in the presence of GMP-PNP (Table 3A). Sufficiently high values of p_n preclude binding of the radioligand to the nth site of R (*i.e.*, $p_n \geq 100$, $\Pi_{j=2}^{n} p_j K_P \gg [P]$). Since the nucleotide causes little or no change in the observed capacity (Figure 4D), its effect is to increase the capacity inferred from the model. The individual estimates of $[R]_t + [S]_t$ are independent of the values of undefined parameters related to the agonists (*i.e.*, K_A, a_j, c_j). There is no set of unconstrained values that avoids a marked increase in $[R]_t + [S]_t$ when R is trivalent or less, the absence of a unique solution notwithstanding; conversely, constraints that prevent the increase also preclude agreement between the model and the data.

The anomaly is avoided if the nth site is not labeled in the absence of GMP-PNP, and the results obtained with p_n fixed at 25 or more are summarized in Table 3B. The fitted curves obtained when R is tetravalent are illustrated in Figure 4 ($-\log p_4 = -1.4$). In the case of divalent R, only 50% of the interacting sites will be labeled at apparently saturating concentrations of the radioligand when p_n is sufficiently large (*i.e.*, $K_P < [P] \ll p_2 K_P$). The corresponding levels of occupancy for trivalent and tetravalent R are 67% and 75%, respectively. Overall occupancy is higher in the presence of noninteracting sites, and the ratios inferred from the present data are 0.54, 0.69, and 0.77 (Table 3B). An inferred ratio of 0.69 also is obtained for S plus tetravalent R when the radioligand labels only half of the interacting sites (*i.e.*, $K_P \simeq p_2 K_P < [P] \ll p_2 p_3 K_P \leq p_2 p_3 p_4 K_P$) and the apparent capacity is expressed relative to that when only p_4 is large (*i.e.*, $K_P \simeq p_2 K_P \simeq p_2 p_3 K_P < [P] \ll p_2 p_3 p_4 K_P$) (Table 3B).

When p_n is near 1 in the absence of nucleotide, the sites labeled only by [^{3}H]quinuclidinylbenzilate are not represented in Scheme 2. When p_n is large, however, the difference in capacity may represent sites that are inaccessible to *N*-[^{3}H]methylscopolamine owing to pronounced negative cooperativity (Wreggett and Wells, 1995). The measured ratio of capacities for *N*-[^{3}H]methylscopolamine and [^{3}H]-

Table 3: Affinities and Capacities for *N*-[^{3}H]Methylscopolamine at Low Ionic Strength: Analysis in Terms of Scheme 2[a]

model	GMP-PNP (mM)	$-\log K_P$	$-\log p_2$	$-\log p_3$	$-\log p_4$	$-\log K_{PS}$	$n[R]_t^b/(n[R]_t+[S]_t)$	capacity for [^{3}H]NMS (±) GMP-PNP[c]	capacity for [^{3}H]NMS apparent[d]	rel SSQ[e]
A. Saturation by *N*-[^{3}H]Methylscopolamine in the Absence of GMP-PNP										
dimer	0.0	9.83 ± 0.02	−0.07 ± 0.03			} 10.51 ± 0.05	0.87	1.78 ± 0.03	1.0	1.00
	0.1	9.71 ± 0.02	−2.40 ± 0.12							
trimer	0.0	9.83 ± 0.05	0.01 ± 0.06	−0.09 ± 0.08		} 10.70 ± 0.13	0.92	1.44 ± 0.02	1.0	0.95
	0.1	9.88 ± 0.04	−0.13 ± 0.06	−1.99 ± 0.15						
tetramer	0.0	9.80 ± 0.08	−0.09 ± 0.16	0.20 ± 0.16	−0.35 ± 0.16	} 10.86 ± 0.13	0.91	1.30 ± 0.02	1.0	0.94
	0.1	9.79 ± 0.07	0.16 ± 0.11	−0.39 ± 0.13	−2.09 ± 0.75					
B. Partial Occupancy by *N*-[^{3}H]Methylscopolamine with and without GMP-PNP										
dimer	0.0	9.49 ± 0.01	−4.00[f]			} 10.65 ± 0.05	0.93	1.01 ± 0.02	0.54	1.00
	0.1	9.75 ± 0.01	−2.46 ± 0.11							
trimer	0.0	9.66 ± 0.03	−0.11 ± 0.04	−1.80[g]		} 10.80 ± 0.12	0.94	1.03 ± 0.02	0.69	0.93
	0.1	9.90 ± 0.02	−0.14 ± 0.05	−1.99 ± 0.13						
tetramer	0.0	9.70 ± 0.07	−0.04 ± 0.12	−0.04 ± 0.15	−1.40[g]	} 10.89 ± 0.14	0.93	1.08 ± 0.02	0.77	0.92
	0.1	9.84 ± 0.06	0.12 ± 0.09	−0.36 ± 0.11	−2.04 ± 0.58					
	0.0	9.56 ± 0.03	−0.26 ± 0.05	−4.00[f]	0.0[f]	} 10.60 ± 0.14	0.95	1.03 ± 0.02	0.69	0.97
	0.1	9.81 ± 0.03	−0.30 ± 0.04	−4.00[f]	0.0[f]					

[a] Estimates of total binding from 12 experiments in buffer A were combined and analyzed in terms of eq 3, with the value of $[P]_b$ computed according to eq 5.1 (dimer), eq 5.2 (trimer), and eq 5.3 (tetramer). Binding was measured at graded concentrations of [^{3}H]NMS (three experiments) or at 0.96−1.05 nM [^{3}H]NMS and graded concentrations of carbachol, arecoline, and methacholine (three experiments each). Each experiment involved parallel assays in the absence of guanyl nucleotide and in the presence of 0.1 mM GMP-PNP; when [^{3}H]NMS was the variable ligand, binding also was measured in the presence of 0.01 mM unlabeled NMS. In all analyses, one value of K_{PS} was common to all of the data; single values of K_P and p_j were common to all data acquired at the same concentration of GMP-PNP, and single values of a_j and c_j were common to the three sets of data acquired with the same agonist at the same concentration of GMP-PNP. The assignments of K_A and K_{AS} were the same as that of a_j when R was di- and trivalent (K_A) or when R was divalent (K_{AS}); otherwise, single values of each parameter were common to the six sets of data acquired with the same agonist. One value of $[R]_t/([R]_t + [S]_t)$ was common to all data, and single values of $[R]_t + [S]_t$ were assigned to data acquired at the same concentration of GMP-PNP in the same experiment. Single values of NS were common to all data from the same experiment. Parametric values listed in the table are defined by at least a shallow minimum in the sum of squares and are largely independent of the values of K_A, a_j, and c_j; the latter are not characterized by unique values in most analyses, particularly when R is tri- or tetravalent. The data and the fitted curves obtained when R is tetravalent (B, $-\log p_4 \leq -1.4$) are illustrated in Figure 4. [b] The fitted values of $[R]_t/([R]_t + [S]_t)$ are as follows: dimer, 0.77 ± 0.01 (A) and 0.87 ± 0.01 (B); trimer, 0.78 ± 0.03 (A) and 0.84 ± 0.03 (B); tetramer, 0.71 ± 0.02 (A), 0.76 ± 0.02 (B, $-\log p_4 \leq -1.4$), and 0.84 ± 0.03 (B, $-\log p_3 = -4.0$). [c] The ratio of capacities (*i.e.*, $[R]_t + [S]_t$) for binding in the presence and absence of GMP-PNP. Values from individual experiments were averaged to obtain the means (±SEM) listed in the table ($N = 12$). [d] The relative apparent capacity for [^{3}H]NMS. (A) The apparent capacity equals $n[R]_t + [S]_t$ in the absence of GMP-PNP. (B) First three analyses: $\{(n-1)[R]_t + [S]_t\}/\{n[R]_t + [S]_t\}$ or $[(n-2)F_R + 1]/[(n-1)F_R + 1]$, where $F_R = [R]_t/([R]_t + [S]_t)$. Last analysis: $\{(n-2)[R]_t + [S]_t\}/\{(n-1)[R]_t + [S]_t\}$ or $[(n-3)F_R + 1]/[(n-2)F_R + 1]$, where $n = 4$. [e] The weighted sum of squares relative to that when R is divalent. [f] The parameter was fixed as shown to preclude binding of the corresponding equivalent of [^{3}H]NMS at the concentrations used in the assays. The weighted sum of squares is independent of the value of p_j under those conditions. [g] The value of p_n is defined by a shallow minimum in the weighted sum of squares and was fixed accordingly.

quinuclidinylbenzilate is 0.66−0.75, which exceeds the value listed in Table 3B for divalent R (*i.e.*, 0.54) but compares favorably with those listed for tri- and tetravalent R. It follows that the cooperative form of the receptor must be at least trivalent if Scheme 2 is to account for the differing capacity of the membranes for the two radioligands.

Alkylated Membranes at Low Ionic Strength. Pretreatment with propylbenzilylcholine mustard reduced the number of interacting sites required for mechanistic consistency in terms of Scheme 2. The binding of carbachol and *N*-[^{3}H]-methylscopolamine to alkylated membranes is illustrated in Figure 5, where the lines represent the best fit of the model with R taken as divalent. It was assumed that the radioligand could label only half of the cooperative sites either with or without GMP-PNP (*i.e.*, $p_2 = 10^4$). The apparent capacity for *N*-[^{3}H]methylscopolamine represents about 60% of the capacity inferred from the model.

The sum of squares is about 7% higher at values of p_2 consistent with saturation of R at the highest concentrations *N*-[^{3}H]methylscopolamine (*i.e.*, $p_2 < 2$), but the fitted curves are almost superimposible with those shown in Figure 5; moreover, the value of p_2 is independent of the nucleotide, and the ratio of capacities inferred from the model is 1.01 ± 0.05. Alkylation therefore eliminated the discrepancy that otherwise emerges in $[R]_t + [S]_t$ when the cooperative form of the receptor is less than tetravalent and the radioligand is assumed to label all of the accessible sites in the absence of GMP-PNP (*cf.* Table 3A).

Native Membranes at High Ionic Strength. The binding of *N*-[^{3}H]methylscopolamine and carbachol in buffer B is illustrated in Figure 6, and the parametric values obtained when R is di- and trivalent are listed in Table 4. Since the Hill coefficient for *N*-[^{3}H]methylscopolamine was indistinguishable from 1, cooperativity unique to the radioligand was fixed accordingly: that is, all values of p_j were taken as 1 when *N*-[^{3}H]methylscopolamine was assumed to label all of the sites (Table 4A); with trivalent R, the value of p_2 was taken as 1.33 when p_3 was assumed to be large (Table 4B). These simplifications are without effect on the goodness of fit regardless of the degree of cooperativity associated with the *n*th equivalent of radioligand. GMP-PNP is therefore without effect on the value of $[R]_t + [S]_t$, in contrast to the discrepancies found with native membranes in buffer A (*cf.* Table 3A). The sum of squares is only 2−5% lower when

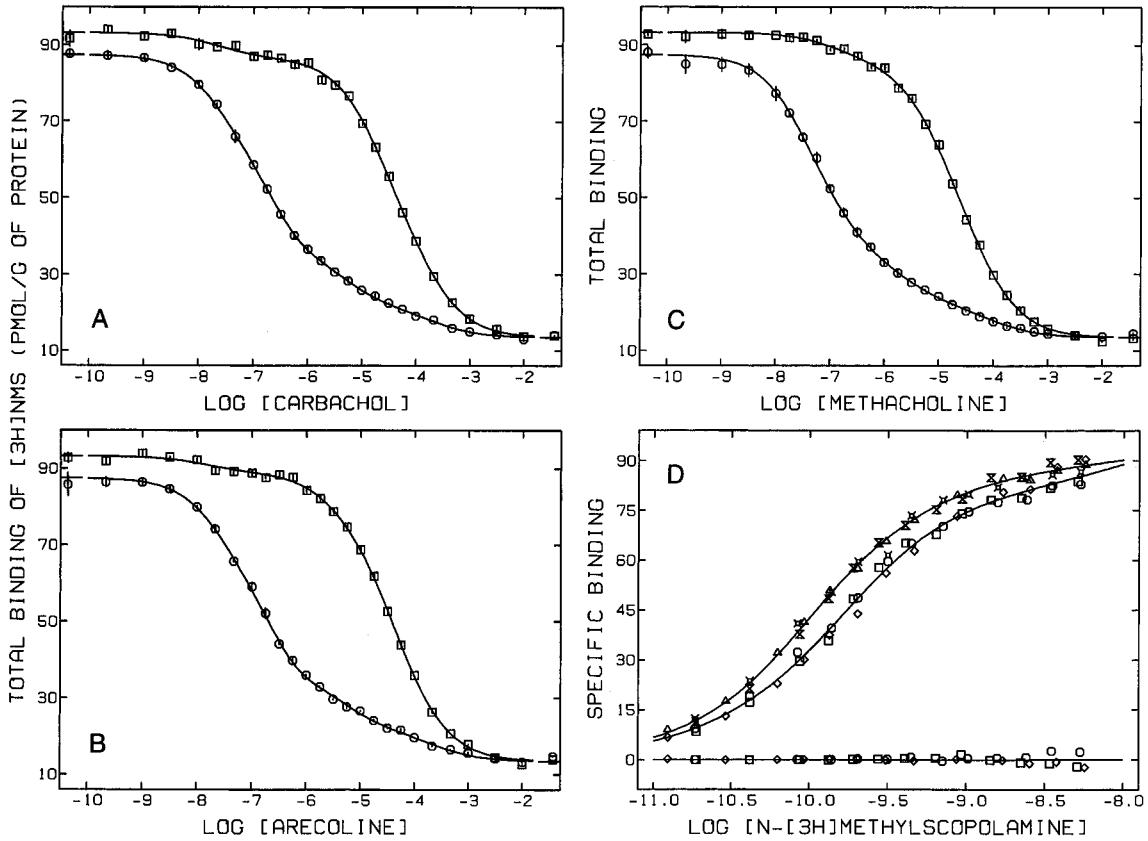

FIGURE 4: Binding of agonists and *N*-[^{3}H]methylscopolamine to native membranes at low ionic strength. Total binding was measured following equilibration of the membranes in buffer A at the concentrations of agonist or [^{3}H]NMS shown on the abscissa. Each panel contains the combined data from three experiments as follows: (A−C) the agonist plus [^{3}H]NMS (0.96−1.05 nM), no GMP-PNP (○), 0.1 mM GMP-PNP (□); (D) [^{3}H]NMS plus 0.1 mM GMP-PNP (⊗, △, hourglass; leftward curve), [^{3}H]NMS alone (○, ◇, □; rightward curve), [^{3}H]NMS plus 0.01 mM unlabeled NMS (○, ◇, □; baseline). In panel D, data from different experiments are represented by different symbols (○, ⊗; ◇, △; □, hourglass). The lines represent the best fit of eq 3 to the combined data; the receptor was assumed to be tetrameric (eq 5.3), and the value of $-\log p_4$ was fixed at -1.4 for binding in the absence of guanyl nucleotide. Further details are described in footnote *a* to Table 3. Values plotted on the ordinate were obtained according to eq 6; for panels A−C, individual values of B'_{obsd} at the same concentration of agonist were averaged, and the mean (±SEM) is shown in the figure. The mean values of $[R]_t + [S]_t$ are 33 ± 1 and 35 ± 1 pmol/g of protein ($N = 12$) for binding in the absence and presence of GMP-PNP, respectively; the mean value of NS is 0.0089 ± 0.0003 ($N = 12$), and the mean concentration of [^{3}H]NMS for the data in panels A−C is 1.01 ± 0.01 nM ($N = 9$). Points shown at the lower and upper ends of the abscissa represent binding in the absence of carbachol and in the presence of 0.01 mM unlabeled NMS, respectively.

R is trivalent rather than divalent, and the two forms of the model yield fitted curves that are virtually superimposible.

Taken alone, the data shown in Figure 6 are consistent with the notion that the cooperative form of the receptor is divalent. If so, R accounts for only 68% or 80% of total capacity depending upon the value of p_2 (*i.e.*, $n[R]_t/(n[R]_t + [S]_t)$, Table 4). The distribution between R and S is defined primarily by the effect of carbachol in the absence of GMP-PNP. Although the different states are not well resolved in buffer B, the fitted values of $n[R]_t/(n[R]_t + [S]_t)$ are significantly less than the corresponding values obtained in buffer A (*i.e.*, 87% and 93%, Table 3) ($P < 0.005$). The analysis therefore implies that the buffer affects the stoichiometry of binding to R and the distribution of sites between R and S. There is no discrepancy between the two buffers if R is tri- or tetravalent: the quantity $n[R]_t/(n[R]_t + [S]_t)$ is essentially undefined when $n > 2$, and the value therefore can be taken as equal to that measured in buffer A.

DISCUSSION

Cooperativity as the Basis for Multiple States of Affinity. There are at least three possible explanations for the dispersion of affinities revealed by agonists at G protein-linked receptors: a heterogeneous mixture of mutually independent and noninterconverting sites [the multisite model; *e.g.*, Munson and Rodbard (1980)], heterogeneity induced by the G protein in a population of mutually independent and otherwise identical sites (the mobile receptor or ternary complex model; De Lean *et al.*, 1980), and cooperative effects among interacting sites. This ambiguity accounts in large measure for lingering uncertainty over the nature of the dispersion itself and, hence, over the mechanism of the allosteric interactions between agonists and guanyl nucleotides.

The genes for five subtypes of muscarinic receptor have been identified (Hulme *et al.*, 1990), and that diversity may account in part for multiple affinities in tissues such as the brain. In the heart, however, northern blots (Peralta *et al.*, 1987; Maeda *et al.*, 1988), immunospecificity (Leutje *et al.*, 1991), and the binding of subtype-specific ligands (Watson *et al.*, 1986a,b; Deighton *et al.*, 1990) all indicate that muscarinic receptors are predominantly, if not exclusively, M_2. Also, guanyl nucleotides, pertussis toxin, N-ethylmaleimide, and some cations all promote an apparent interconversion of cardiac muscarinic receptors from one state to another. Similarly, agonists appear to regulate the distribu-

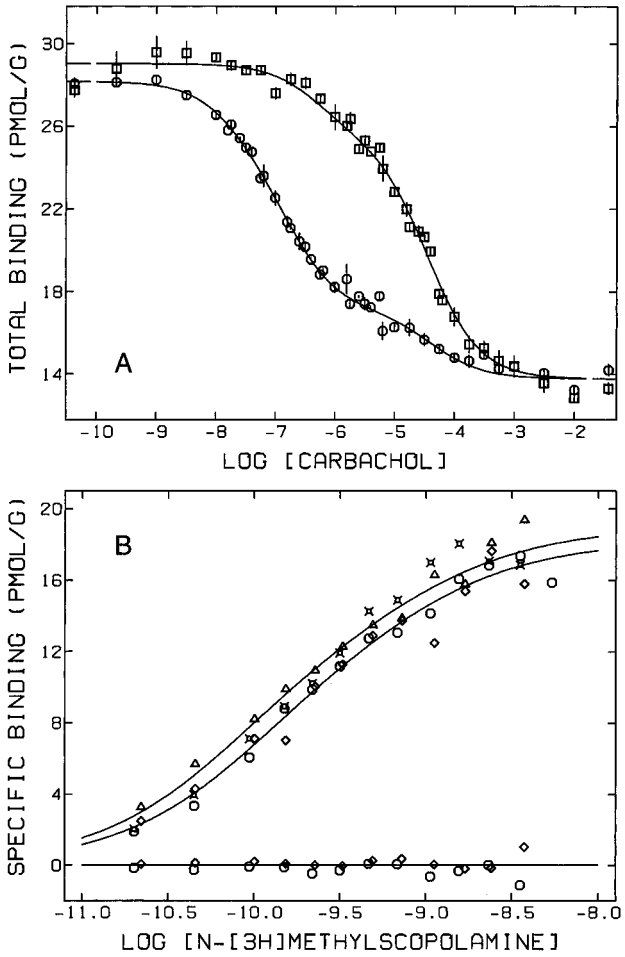

FIGURE 5: Binding of carbachol and *N*-[^{3}H]methylscopolamine to alkylated membranes at low ionic strength. Total binding was measured following equilibration of the membranes in buffer A. Each panel contains the combined data from three (A) or two (B) experiments as follows: (A) carbachol plus [^{3}H]NMS (1.01, 1.03, or 0.59 nM), no GMP-PNP (○), 0.1 mM GMP-PNP (□); (B) [^{3}H]-NMS plus 0.1 mM GMP-PNP (⊗, △; leftward curve), [^{3}H]NMS alone (○, ◇; rightward curve), [^{3}H]NMS plus 0.01 mM unlabeled NMS (○, ◇; baseline). In panel B, data from different experiments are represented by different symbols (○, ⊗; ◇, △). The lines represent the best fit of eq 3 to the combined data; the receptor was assumed to be dimeric, and the value of $[P]_b$ in eq 3 was computed according to eq 5.1. One value of K_{PS} was common to all of the data, and one value of K_{AS} was common to all data acquired at graded concentrations of carbachol. One value of K_P was common to all data acquired at the same concentration of GMP-PNP. Single values of K_A, a_2, and c_2 were common to all data acquired in the presence of carbachol at the same concentration of GMP-PNP. The value of $-\log p_2$ was fixed at -4.0 throughout; other parameters unique to the radioligand were well-defined by the data, and the fitted values are as follows: $-\log K_P = 9.72 \pm 0.03$ (no GMP-PNP) or 9.85 ± 0.04 (+GMP-PNP), $-\log K_{PS} = 9.12 \pm 0.12$ (±GMP-PNP). One value of $[R]_t/([R]_t + [S]_t)$ was common to all of the data, and the fitted estimate is 0.67 ± 0.03; the corresponding value of $n[R]_t/(n[R]_t + [S]_t)$ is 0.80. The fraction of all sites labeled at the highest concentrations of the radioligand is therefore 0.60. Values of $[R]_t + [S]_t$ and NS were assigned as described in footnote *a* to Table 3; the means for the five experiments represented in the figure are 18 ± 2 (no GMP-PNP) and 19 ± 2 (0.1 mM GMP-PNP) pmol/g of protein for $[R]_t + [S]_t$ and 0.0092 ± 0.0005 for NS. Estimates of B_{obsd} were adjusted according to eq 6 to obtain the mean (±SEM) (A) or the individual values (B) plotted on the ordinate; the concentration of [^{3}H]NMS was taken as 1.0 nM for the data in panel A. Further details are described in the legend to Figure 4.

tion of sites among the different states under some conditions (Wong *et al.*, 1986). The multisite model therefore is

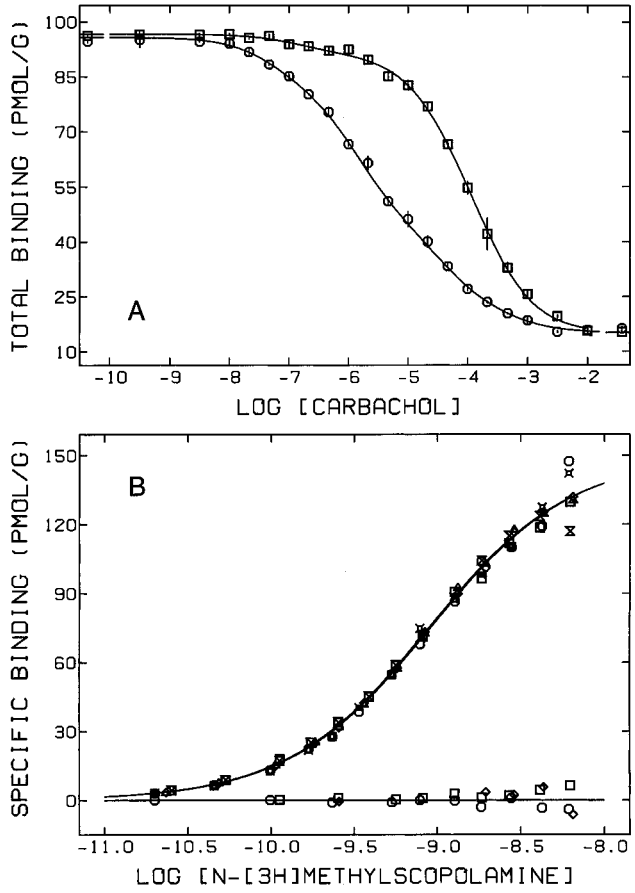

FIGURE 6: Binding of carbachol and *N*-[^{3}H]methylscopolamine to native membranes at high ionic strength. Total binding was measured following equilibration of the membranes in buffer B. Each panel contains the combined data from three experiments as follows: (A) carbachol plus [^{3}H]NMS (1.02−1.14 nM), no GMP-PNP (○), 0.1 mM GMP-PNP (□); (B) [^{3}H]NMS alone (○, ◇, □), [^{3}H]NMS plus 0.1 mM GMP-PNP (⊗, △, hourglass), [^{3}H]NMS plus 0.01 mM unlabeled NMS (○, ◇, □; baseline). In panel B, data from different experiments are represented by different symbols (○, ⊗; ◇, △; □, hourglass). The lines represent the best fit of eq 3 to the combined data; the receptor was assumed to be trimeric (eq 5.2), and the value of $-\log p_3$ was fixed at -4.0 throughout. Further details are described in footnote *a* to Table 4. Estimates of B_{obsd} were adjusted according to eq 6 to obtain the mean (±SEM) (A) or the individual values (B) plotted on the ordinate. The mean value of $[R]_t + [S]_t$ is 81 ± 3 pmol/g of protein for binding either with or without GMP-PNP ($N = 6$); the mean value of NS is 0.0071 ± 0.0002 ($N = 6$), and the mean concentration of [^{3}H]NMS for the data in panel A is 1.07 ± 0.04 nM ($N = 3$). Further details are described in the legend to Figure 4.

mechanistically untenable, despite its widespread use in analyses of the data.

The quantitative implications of the mobile receptor model have been examined by Lee *et al.* (1986), who concluded that the original proposal is inconsistent with the binding properties of muscarinic and other G protein-linked receptors. Some of the problems can be resolved by expanded versions of the model, allowing in particular for multiple subtypes of G proteins and a subpopulation of G protein-inaccessible receptors. As described in the accompanying paper (Green *et al.*, 1997), however, at least one such scheme cannot account for the effects of GMP-PNP or propylbenzilylcholine mustard; furthermore, it yields wholly inconsistent views of the system in studies with *N*-[^{3}H]methylscopolamine on the one hand and [^{35}S]GTPγS on the other. Such schemes also fail to account for the levels of amplification inferred from

Table 4: Affinities and Capacities for *N*-[^{3}H]Methylscopolamine at High Ionic Strength. Analysis in Terms of Scheme 2[a]

model	GMP-PNP (mM)	$-\log K_P$	$-\log p_2$	$-\log p_3$	$-\log K_{PS}$	$n[R]_t^b/(n[R]_t+[S]_t)$	capacity for [^{3}H]NMS (±) GMP-PNP[c]	capacity for [^{3}H]NMS apparent[d]	rel SSQ[e]
A. Saturation by *N*-[^{3}H]Methylscopolamine									
dimer	0.0	9.02 ± 0.10	0.0[f]		9.13 ± 0.20	0.68	0.99 ± 0.01	1.0	1.00
	0.1	9.04 ± 0.10	0.0[f]						
trimer	0.0	9.03 ± 0.04	0.0[f]	0.0[f]	9.27 ± 0.27	0.92	1.00 ± 0.01	1.0	0.98
	0.1	9.05 ± 0.04	0.0[f]	0.0[f]					
B. Partial Occupancy by *N*-[^{3}H]Methylscopolamine									
dimer	0.0	8.73 ± 0.12	−4.0[g]		9.12 ± 0.23	0.80	0.99 ± 0.01	0.60	1.00
	0.1	8.75 ± 0.12	−4.0[g]						
trimer	0.0	8.89 ± 0.04	−0.125[f]	−4.0[g]	8.97 ± 0.52	0.94	1.00 ± 0.01	0.69	0.95
	0.1	8.91 ± 0.04	−0.125[f]	−4.0[g]					

[a] Estimates of total binding from six experiments in buffer B were combined and analyzed in terms of eq 3, with the value of $[P]_b$ computed according to eq 5.1 (dimer) and eq 5.2 (trimer). Binding was measured at graded concentrations of [^{3}H]NMS (three experiments) or at 1.02−1.14 nM [^{3}H]NMS and graded concentrations of carbachol (three experiments), both in the absence of guanyl nucleotide and in the presence of 0.1 mM GMP-PNP. In all analyses, one value of K_{PS} was common to all of the data, and one value of K_{AS} was common to the six sets of data acquired with carbachol; single values of K_P and p_j were common to all data acquired at the same concentration of GMP-PNP, and single values of a_j and c_j were common to the three sets of data acquired with carbachol and at the same concentration of GMP-PNP. Further details are given in footnote *a* to Table 3. The data and the fitted curves obtained when R is trivalent (B, $-\log p_3 = -4.0$) are illustrated in Figure 6. [b] The fitted values of $[R]_t/([R]_t + [S]_t)$ obtained when R is divalent are 0.52 ± 0.08 (A) and 0.67 ± 0.08 (B). The parameter is not well-defined when R is trivalent, and the value was fixed at that obtained from the data acquired at low ionic strength (Table 3) (*i.e.*, A, 0.78; B, 0.84). [c] The ratio of capacities (*i.e.*, $[R]_t + [S]_t$) for binding in the presence and absence of GMP-PNP. Values from individual experiments were averaged to obtain the means (±SEM) listed in the table ($N = 6$). [d] The relative apparent capacity for [^{3}H]NMS. (A) The apparent capacity equals $n[R]_t + [S]_t$. (B) $\{(n-1)[R]_t + [S]_t\}/\{n[R]_t + [S]_t\}$ or $[(n-2)F_R + 1]/[(n-1)F_R + 1]$, where $F_R = [R]_t/([R]_t + [S]_t)$. [e] The weighted sum of squares relative to that when R is divalent. [f] The values of p_j were fixed as shown, in agreement with the apparent homogeneity of the sites for [^{3}H]NMS (*i.e.*, $n_H = 1$). [g] The value of p_n was fixed to preclude binding of the corresponding equivalent of [^{3}H]NMS at the concentrations used in the assays.

the agonist-promoted turnover of guanyl nucleotides, and they require a degree of compartmentalization that may occur in native membranes but seems unlikely in solubilized or reconstituted preparations. These discrepancies cast doubt on the underlying notion of a ligand-regulated equilibrium between free and G protein-coupled receptors [see Green *et al.* (1997), and references cited therein].

In schemes based on the mobile receptor model, multiple affinities arise wholly or in part from mutual depletion of the receptor and G protein as the agonist promotes formation of the RG complex. Binding therefore is not described by a rational function, in contrast to the multisite model and models based on cooperativity (Wells, 1992). It follows that the dispersion seen in the semilogarithmic binding curve relates only indirectly to the multiple states and affinities of the receptor; for example, the first derivative may contain a single maximum regardless of the difference in the affinity of the ligand for R and RG. One consequence of this situation is that the observed potencies of agonists and the apparent distribution of sites among different states ought to depend upon the local concentrations and mutual affinity of the interacting proteins (Lee *et al.*, 1986). This prediction differs from the widespread observation that estimates of affinity from the multisite model are largely unaffected by conditions that cause interconversion in membranes, in vesicles, and in solution [*e.g.*, Table 2; Ikegaya *et al.*, 1990; Sinkins *et al.*, 1993; see also Wong *et al.* (1986) and references cited therein]; moreover, the affinity spectrum for the binding of isoproterenol to β-adrenergic receptors is manifestly bimodal (Tobler and Engel, 1983).

The consistency achieved with the multisite model suggests that the mechanistically correct model is itself a rational function. One such possibility is represented by Scheme 2, which comprises two independent forms of the receptor: a multivalent form that supports cooperative effects among interacting sites (R) and a monovalent form in which the sites are mutually independent (S). The former is modeled as an extension of the Adair equation for two competing ligands, and the latter is included to account for the failure of propylbenzilylcholine mustard to eliminate the sites of lowest affinity for agonists.

Scheme 2 provides an excellent description of the present data, and it offers a mechanistically consistent view of effects that appear contradictory or paradoxical in terms of alternative proposals. Multiple states of affinity are a manifestation of cooperativity and hence intrinsic to the receptor; accordingly, the model can account for the retention of native properties under conditions that otherwise are expected to effect profound changes in the behavior of the system. The effects of GMP-PNP can be attributed wholly to changes in affinity, particularly as determined by the degree of cooperativity at various levels of occupancy. Similarly, the differential capacity for [^{3}H]quinuclidinylbenzilate and *N*-[^{3}H]-methylscopolamine can be attributed to pronounced negative cooperativity in the binding of the latter. Whereas the cooperative form of the receptor must be at least trivalent in native membranes, it can be divalent in alkylated membranes that retain only 21% of the native capacity. The difference is consistent with the notion that propylbenzilylcholine mustard has reduced the number of functional, interacting sites within a structurally stable oligomer.

The possibility of cooperative effects has been noted previously or can be inferred from the results of previous investigators. Henis and Sokolovsky (1983) have described apparently noncompetitive behavior in the binding of antagonists to muscarinic receptors in membranes from rat adenohypophysis, and the effects were rationalized in terms of cooperativity between two interacting sites. Also, Hill coefficients of 1.4−1.5 have been reported for the specific binding of [^{3}H]quinuclidinylbenzilate to cardiac membranes

(Mattera *et al.*, 1985; Boyer *et al.*, 1986); the inhibitory behavior of muscarinic agonists was interpreted in terms of a static mixture of noncooperative and cooperative bivalent receptors, although the effect of GMP-PNP emerged in part as an interconversion between the two forms (Mattera *et al.*, 1985). Hill coefficients of 1.26 and 1.54 have been found for the inhibitory effect of two histaminic ligands on the specific binding of [^{3}H]histamine to two classes of sites in membranes of guinea pig cortex; moreover, the inhibitory behavior of ligands that recognized two classes of sites appeared to violate microscopic reversibility unless the data were analyzed in terms of cooperativity (Sinkins and Wells, 1993). Studies on the photocycling of bacteriorhodopsin have suggested an asymmetric cooperativity based on a trimer (Tokaji, 1993). The possibility that cooperativity derives from an oligomeric receptor is consistent with the binding properties of complementary chimeras of α_2 adrenergic and m3 muscarinic receptors coexpressed in COS-7 cells (Maggio *et al.*, 1993). No binding was observed when either protein was expressed alone, suggesting that a functional receptor required structural elements from at least one equivalent of each chimera. Since the Hill coefficient reported for carbachol is 0.64, it follows that the functional oligomer was at least a tetramer.

Number of Interacting Sites on the Cooperative Form of the Receptor. The estimated stoichiometry of binding is linked to the low capacity for *N*-[^{3}H]methylscopolamine, which labeled only 66−75% of the sites recognized by [^{3}H]-quinuclidinylbenzilate. Two possible explanations for that difference have been considered here: the unlabeled sites may be physically inaccessible to hydrophilic radioligands, as suggested previously [*e.g.*, Brown and Goldstein (1986)], or *N*-[^{3}H]methylscopolamine may be negatively cooperative at high concentrations.

Compartmentalization implies that the extra sites labeled by [^{3}H]quinuclidinylbenzilate are not represented in Scheme 2. If the observed capacity for *N*-[^{3}H]methylscopolamine represents all sites accessible to both radioligands (*i.e.*, $p_j \simeq 1$ for all j, Table 3A), the effect of GMP-PNP on agonists places a lower limit on the stoichiometry for binding to R. At low ionic strength, at least four interacting sites are required to avoid an anomalous, nucleotide-dependent increase in capacity as inferred from the model. The inferred increase is small when R is tetravalent, and the fitted curves obtained when such an effect is disallowed are not appreciably different from those illustrated in Figure 4. The effect on $[R]_t + [S]_t$ is an artifact in which GMP-PNP appears to induce negative cooperativity in the binding of *N*-[^{3}H]-methylscopolamine. As described below, it arises from constraints imposed by the relative abundance of the different states recognized by agonists and by the high level of occupancy achieved by the radioligand: in the absence of agonist, the labeled sites represented about 90% of the apparent capacity.

In contrast to the notion of restricted access, several observations suggest that all binding of both radioligands occurs within the context of Scheme 2. Purified M_2 receptors from porcine atria reveal a differential capacity similar to that described here, and apparently cooperative effects have been identified between the sites labeled by both radioligands and those specific for [^{3}H]quinuclidinylbenzilate (Wreggett and Wells, 1995). Essentially the same pattern has been found with M_2 receptors in porcine sarcolemmal membranes (Pyo and Wells, 1996), and the Hill coefficient of 1.3−1.4 obtained for [^{3}H]quinuclidinylbenzilate in those preparations[6] also is suggestive of interacting sites [*cf.* Mattera *et al.* (1985) and Boyer *et al.* (1986)]. The evidence for noncompetitive effects argues in favor of negative cooperativity as the cause of the low capacity for *N*-[^{3}H]methylscopolamine. That occurs with values of p_n such that binding to the corresponding sites is precluded with or without GMP-PNP (Table 3B). A multivalent receptor also may be intrinsically asymmetric with respect to the ligand, a possibility that cannot be ruled out with the present data. The specific radioactivity of the probe is the same throughout, and each asymmetric arrangement has a symmetric equivalent when the system is cooperative.

If the differential capacity denotes negative cooperativity exclusive to *N*-[^{3}H]methylscopolamine, the number of interacting sites is determined largely by the magnitude of the difference. The value of 25−34% found in hamster myocardium is too small for dimeric R but approximates that expected for a trimer or a tetramer if cooperativity excludes only the last equivalent of *N*-[^{3}H]methylscopolamine. Tetrameric R also suggests a further possibility in which cooperativity excludes the last equivalent of [^{3}H]quinuclidinylbenzilate and the last two equivalents of *N*-[^{3}H]methylscopolamine. Although a clear distinction between tri- and tetravalent R is not possible with the present data, purified M_2 receptors appear to be at least tetravalent (Wreggett and Wells, 1995). Moreover, the apparent capacity for *N*-[^{3}H]-methylscopolamine can be about 50% of that for [^{3}H]-quinuclidinylbenzilate in myocardial membranes and after purification (Brown and Goldstein, 1986; Wreggett and Wells, 1995), which implies an even number of interacting sites. It follows that R is at least tetravalent in hamster myocardium if the stoichiometry of binding is the same in all preparations. Variations in relative capacity may arise from differences in cooperativity from preparation to preparation.

At higher ionic strength, GMP-PNP is without effect on the cooperativity of *N*-[^{3}H]methylscopolamine, and divalent R is sufficient to describe the data. The success of the simpler model is due primarily to the affinity of the radioligand (log $EC_{50} = -9.1$), which was about 6-fold weaker than at lower ionic strength (log $EC_{50} \leq -9.88$). Since only 50% of the observed sites were labeled at higher ionic strength, the model is comparatively unconstrained. A less constrained model is also less informative, but it seems likely that the nature of the system is the same in both buffers: three classes of sites were observed throughout, and the nucleotide appeared to act selectively on F_j and K_{A2} (Table 2). It is implicit in Scheme 2 that the buffer is without effect on the distribution of sites between R and S; if so, the cooperative form of the receptor must be at least trivalent.

Receptors in the alkylated membranes also can be described in terms of divalent R, but the assays were performed at low ionic strength. Most of the observable sites were labeled by *N*-[^{3}H]methylscopolamine at the concentration used, and the success of the simpler model is due largely to changes effected by the mustard in the binding of carbachol in the presence of GMP-PNP. In terms of Scheme 1, there were proportionately more low-affinity sites, and there was

[6] N. Pyo and J. W. Wells, unpublished observations.

no nucleotide-dependent increase in K_{Aj} at the sites of medium affinity (Table 2). Partial inactivation of a tetravalent receptor is expected to yield a mixture of species, and a description of such a system in terms of Scheme 2 is largely empirical. If the mustard acts randomly, however, tri- and tetravalent species will contribute fewer than 10% of the functional sites at levels of alkylation exceeding about 75%. Such a reduction in the average number of functionally viable, interacting sites is consistent with the good agreement obtained between the data and Scheme 2 when R is only divalent.

The apparent capacity of alkylated membranes for *N*-[^{3}H]-methylscopolamine represents 60% of the inferred capacity in terms of Scheme 2, assuming that divalent R binds only one equivalent of the radioligand (*i.e.*, $-\log p_2 = -4.0$, Figure 5). The corresponding value for native membranes is 69−77% when R is tri- or tetravalent (Table 3B), and the apparent capacity for *N*-[^{3}H]methylscopolamine was 66−75% of that for [^{3}H]quinuclidinylbenzilate. These values are in good agreement with the results of similar studies on sarcolemmal membranes from porcine atria, where the binding of both radioligands has been measured before and after alkylation: when the apparent capacity for *N*-[^{3}H]-methylscopolamine was reduced to 21% of native levels, the relative capacity for *N*-[^{3}H]methylscopolamine and [^{3}H]-quinuclidinylbenzilate was reduced from 0.76 ± 0.01 to 0.57 ± 0.03 ($N = 3$) (Pyo and Wells, 1996).

Constraints on Scheme 2. Despite a comparatively large number of parameters, some of which may be undefined, the model is limited in its versatility under some conditions. Binding patterns that lie outside those limits can lead to anomalies such as the nucleotide-dependent effects on $[R]_t + [S]_t$ described above (Table 3A). Scheme 2 is particularly restricted by two aspects of the present data: the effect of GMP-PNP on the binding of agonists and the concentration of *N*-[^{3}H]methylscopolamine used in those assays. The effects of such conditions on the behavior of the model are illustrated in Figures 7 and 8, where the curves have been computed for divalent and tetravalent R, respectively. All sites are of equal affinity for the radioligand in each case (*i.e.*, $p_j = 1$).

At lower concentrations of the probe (*e.g.*, $[P] = K_P/10$), either form of the model can predict the inhibitory pattern typically reported for an agonist at different concentrations of a guanyl nucleotide: that is, the nucleotide effects an apparent interconversion of sites from higher to lower affinity for the agonist, and there is little or no change in affinity *per se* as estimated empirically in terms of Scheme 1 (curves a−f in Figures 7A and 8A) [*e.g.*, Kent *et al.* (1980)]. In the examples shown, the distinctly biphasic nature of the inhibition reflects a 1000-fold difference in affinity between successive equivalents of unlabeled ligand.[7] The individual curves in each panel differ only in the degree of cooperativity between the unlabeled ligand and the probe (*i.e.*, c_j), which determines the position of the plateau that defines the apparent distribution of sites in terms of Scheme 1 (*i.e.*, F_j) [see also Mattera *et al.* (1985)]. As the cooperative effect becomes more positive (curves g and h), the model predicts a bell-shaped pattern that cannot be obtained from a system of ligands and mutually independent sites at thermodynamic equilibrium.

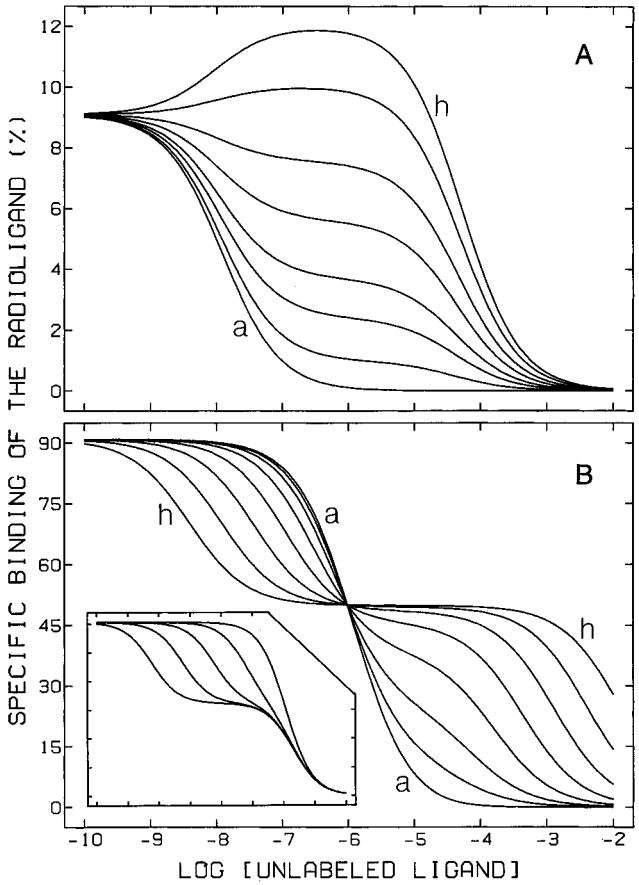

FIGURE 7: Behavior of a divalent cooperative receptor. The lines were simulated according to Scheme 2 ($n = 2$, eq 5.1, $[S]_t = 0$) for an unlabeled ligand at two concentrations of a radiolabeled probe (A, $[P] = K_P/10$; B, $[P] = 10K_P$). Successive equivalents of the unlabeled ligand exhibit negative cooperativity ($-\log a_2 < 0$); the radioligand itself is not cooperative ($\log p_2 = 0$). The values of $-\log K_A$ and $-\log a_2$ are 7.7 and −3.0, respectively, for all curves in panel A and in the outer frame of panel B. The values of $-\log c_2$ in panel A are as follows: a, −3.0; b, −0.7; c, −0.3; d, −0.1; e, 0.1; f, 0.25; g, 0.4; and h, 0.5. Those in the outer frame of panel B are as follows: a, −3.0; b, −1.5; c, −1.0; d, −0.5; e, 0; f, 0.5; g, 1.0; and h, 1.5. Lines in the inset to panel B were simulated with $-\log c_2$ taken as 0.5; the values of $-\log K_A$ and $-\log a_2$ are as follows, from left to right: 8.5 and −3.0, 7.5 and −2.0, 6.5 and −1.0, 5.5 and 0, and 4.5 and 1.0. The abscissa shows the free concentration of the unlabeled ligand, and values plotted on the ordinate represent bound radioligand relative to the total concentration of sites taken as 100.

At higher concentrations of the probe (*e.g.*, $[P] = 10K_P$), changes in c_j alone are unable to mimic the observed effect of guanyl nucleotides on the binding of agonists. If R is only divalent, there is an upper limit of 0.5 on the fraction of sites ostensibly of low affinity (Figure 7B); moreover, the agonist becomes more potent at the high-affinity sites ($IC_{50(1)}$) and less potent at the low-affinity sites ($IC_{50(2)}$) as cooperativity between the two ligands is increased from negative ($c_2 > 1$) to positive ($c_2 < 1$). The reduction in $IC_{50(1)}$ arises from increased affinity for the agonist at one

[7] With a divalent receptor (Figure 7A), the difference in affinity derives from negative cooperativity between the first and second equivalents of the unlabeled ligand (*i.e.*, $a_2 = 10^3$). A tetravalent receptor can yield virtually the same pattern with various combinations of parameters. In the example shown (Figure 8A), negative cooperativity is associated primarily with the third and fourth equivalents of the unlabeled ligand (*i.e.*, $a_2 = 5.6$, $a_3 = 1.5$, $a_4 = 10^3$). The curves were simulated to mimic a single class of sites for the first two equivalents of the ligand; since the model was formulated with microscopic binding constants, the values of a_2 and a_3 exceed 1.

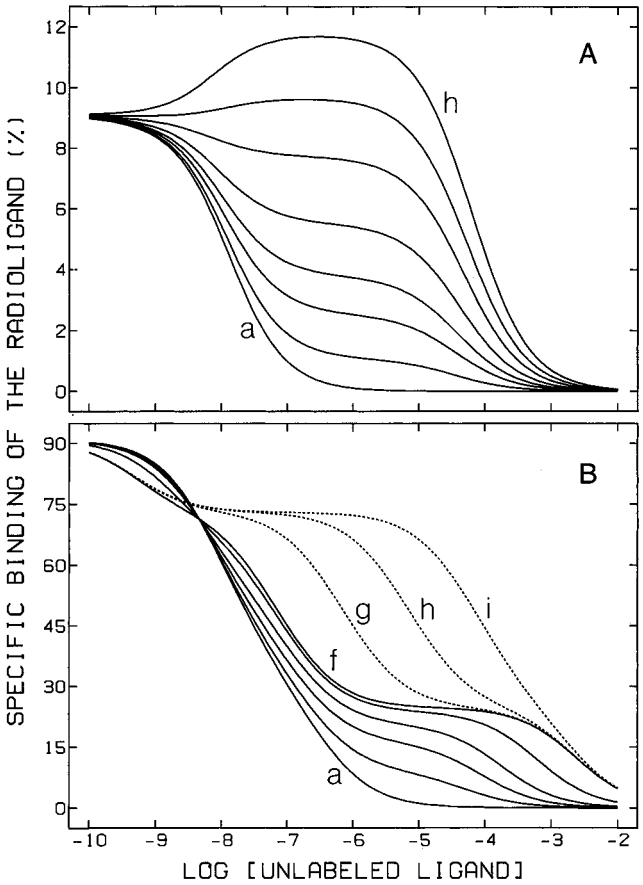

FIGURE 8: Behavior of a tetravalent cooperative receptor. The lines were simulated according to Scheme 2 ($n = 4$, eq 5.3, $[S]_t = 0$) for an unlabeled ligand at two concentrations of a radiolabeled probe (A, $[P] = K_P/10$; B, $[P] = 10K_P$). Each equivalent of the unlabeled ligand is negatively cooperative with respect to the next ($-\log a_j < 0$), with the major change occurring between the third and fourth equivalents (*i.e.*, a_4); the radioligand itself is not cooperative ($\log p_j = 0$). Parametric values common to the solid lines in both panels are as follows: $-\log K_A = 9.0$, $-\log a_2 = -0.75$, $-\log a_3 = -0.17$, $-\log a_4 = -3.0$, $-\log c_2 = 0.13$, and $-\log c_3 = 0.12$. The values of $-\log c_4$ in panel A are as follows: a, −3.0; b, −0.6; c, −0.2; d, 0; e, 0.2; f, 0.4; g, 0.55; and h, 0.7. The values of $-\log c_4$ for the solid lines in panel B are as follows: a, −3.0; b, −1.5; c, −1.0; d, −0.6; e, 0; and f, 0.6. The dotted lines in panel B illustrate the effect of a shift in negative cooperativity from a_4 to a_2 at a relatively low value of c_4 ($-\log c_4 = 0.6$, *cf.* curve f). The values of $-\log a_2$ and $-\log a_4$ are as follows: g, −1.75 and −2.0; h, −2.75 and −1.0; and i, −3.75 and 0. Other details are as described in the legend to Figure 7.

site when the other is occupied by the radioligand; similarly, the increase in $IC_{50(2)}$ arises from increased affinity for the radioligand at one site when the other site is occupied by the agonist. The effects of c_2 on IC_{50} can be offset by concomitant changes in K_A and a_2 (inset, Figure 7B), but labeling associated with $IC_{50(2)}$ remains limited to half of $[R]_t$ or less. Such adjustments therefore cannot account for the mix of high- and low-affinity sites observed experimentally in the presence of GMP-PNP (Table 2).

These limitations on divalent R can be overcome by values of p_2 such that only one of the two interacting sites is deemed to be labeled (*e.g.*, $[P] = 10K_P$; $[P] \ll p_2K_P$). Since the species RP_2 does not occur, specific binding comprises only RP and ARP. The conditions therefore resemble those at lower concentrations of the probe, and the system can mimic the behavior shown in Figure 7A. Since the apparent capacity for *N*-[^{3}H]methylscopolamine was unaffected by GMP-PNP, a nucleotide-mandated increase in p_2 is associated with a spurious increase in the computed value of $[R]_t + [S]_t$ (Table 3A).

Tetravalent R gives a pattern analogous to that obtained with the simpler model. The solid lines in Figure 8B differ in the degree of cooperativity between the unlabeled ligand and the probe when forming the tetraliganded species (*i.e.*, c_4). As the cooperativity is increased from negative ($c_4 > 1$) to positive ($c_4 < 1$), the fraction of sites ostensibly of lowest affinity for the unlabeled ligand increases from 0 to an upper limit of 0.25. Similar variations in c_3 and c_2 reveal limits of 0.50 and 0.75, respectively, and the binding profile therefore may comprise up to four inflections. The effects on IC_{50} parallel those illustrated in Figure 7B, and changes in c_j alone cannot mimic the effect of GMP-PNP. At larger values of n, however, concomitant changes in K_A and a_j enable the model to accommodate high-affinity sites that coexist with the nucleotide. This flexibility is illustrated by the dotted lines in Figure 8B, where negative cooperativity intrinsic to the unlabeled ligand is shifted incrementally from the third and fourth equivalents (a_4) to the first and second equivalents (a_2). With the three agonists used in the present investigation, the prevalence of high- and medium-affinity sites in the presence of GMP-PNP is too low for tetravalent R alone, and a pentavalent or larger species would be required if all sites occurred in cooperative arrays. Approximately 15% of the receptors appear to be noncooperative, however, and the sites of higher affinity for agonists therefore represent a correspondingly greater fraction of those identified as cooperative.

If the lower capacity for *N*-[^{3}H]methylscopolamine derives from negative cooperativity, the apparent level of occupancy exceeds the true level with or without GMP-PNP. Since the value of p_n is large throughout, no change is required for the model to account for the binding of agonists in the presence of GMP-PNP, and an untoward increase in $[R]_t + [S]_t$ is avoided (Table 3B). A good fit requires negative cooperativity at only the last equivalent of the radioligand regardless of the number of interacting sites. With divalent R, a high value of p_2 reduces the level of occupancy from 90% to about 50% at 1 nM *N*-[^{3}H]methylscopolamine (*cf.* Figure 7). The reduction is less at higher values of n, but there is a corresponding decrease in the discrepancy between the model and the binding of carbachol in the presence of GMP-PNP (*cf.* Figure 8B).

Multiple States of the Unliganded Receptor and the Nature of the Effect of Guanyl Nucleotides. G protein-mediated systems often exhibit spontaneous activity that can be inhibited by antagonists (Schütz and Freissmuth, 1992). Examples at different levels of response include the GTPase activity of the G protein (Costa and Herz, 1989), the regulation of second messengers in preparations of wild-type and constitutively active receptors [*e.g.*, Kjelsberg *et al.* (1992) and Chidiac *et al.* (1994)], and the atrial inotropic response in transgenic mice with myocardial overexpression of the β_2 receptor (Bond *et al.*, 1995). In such systems, the receptor appears to interconvert spontaneously between an inactive state favored by antagonists and an active state favored by agonists (Chidiac *et al.*, 1994; Leff, 1995).

The notion of a ligand-regulated equilibrium between two states is consistent with the general pattern revealed in binding studies. Guanyl nucleotides are found almost universally to reduce the apparent affinity of G protein-linked

Scheme 3[a]

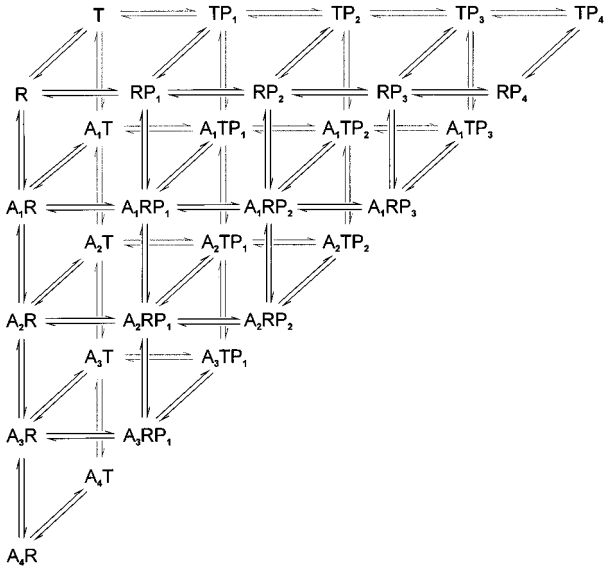

[a] The cooperative form of the receptor illustrated in Scheme 2 can exist in two, spontaneously interconverting states designated R and T. The distribution of sites in the absence of ligand is given by the equilibrium constant K_{RT} (*i.e.*, [R]/[T] = K_{RT}), and other parameters are analogous to those of Scheme 2 (*i.e.*, K_{PR}, K_{PT}, K_{AR}, K_{AT}, p_{Rj}, p_{Tj}, a_{Rj}, a_{Tj}, c_{Rj}, c_{Tj}).

receptors for agonists. The apparent affinity for antagonists often is unaffected (*e.g.*, Figure 6B) but can be increased under some conditions [*e.g.*, Figure 4D, Burgisser *et al.* (1982), and Wreggett and De Lean (1984)]. Conversely, agonists reduce the apparent affinity of receptor-linked G proteins for GDP [*e.g.*, Bennett and Dupont (1985), Tota *et al.* (1987), Hilf *et al.* (1989), and Chidiac and Wells (1992)], while antagonists seem to cause an increase in at least some cases [*e.g.*, Hilf and Jakobs (1992)].

Only one state is accessible to the vacant receptor in Scheme 2 [see also Adair (1925) and Koshland *et al.* (1966)], and a framework common to binding and response is not self-evident. An expansion of the model is shown in Scheme 3, where the receptor is assumed to interconvert spontaneously between two states designated R and T. Such an arrangement follows the approach described by Monod *et al.* (1965), less their restriction that binding is intrinsically independent at each site. In the original proposal, homotropic effects were attributed exclusively to the conservation of symmetry and the difference in the affinity of the ligand for R and T. Those constraints allow only for positive cooperativity; otherwise, the model also can predict negative cooperativity. A system such as Scheme 3 can account for the several phenomena that seem likely to share a common mechanistic basis: namely, the occurrence of constitutive activity, the differential effects of agonists and inverse agonists, the multiple states of affinity, and the effects of guanyl nucleotides.

In terms of Scheme 3, G proteins and guanyl nucleotides can be regarded as allosteric effectors that shift the equilibrium between R and T. In the absence of an explicit mechanism for such effects, the shift can be modeled empirically as a change in the corresponding equilibrium constant (*i.e.*, K_{RT} = [R]/[T]). Changes in the binding of receptor-specific ligands then arise from differences in the cooperativity of R and T (*i.e.*, $p_{Rj} \neq p_{Tj}$, $a_{Rj} \neq a_{Tj}$, or $c_{Rj} \neq c_{Tj}$), in the affinity of the vacant receptor (*i.e.*, $K_{PR} \neq K_{PT}$, or $K_{AR} \neq K_{AT}$), or in both. The equilibrium between R and T also will be regulated by agonists and antagonists to the extent that the ligand differs in its affinity for the two states at each level of occupancy. Scheme 3 therefore can accommodate G protein-mediated effects on binding and, within the same framework, the functional differences among agonists, antagonists, and inverse agonists.

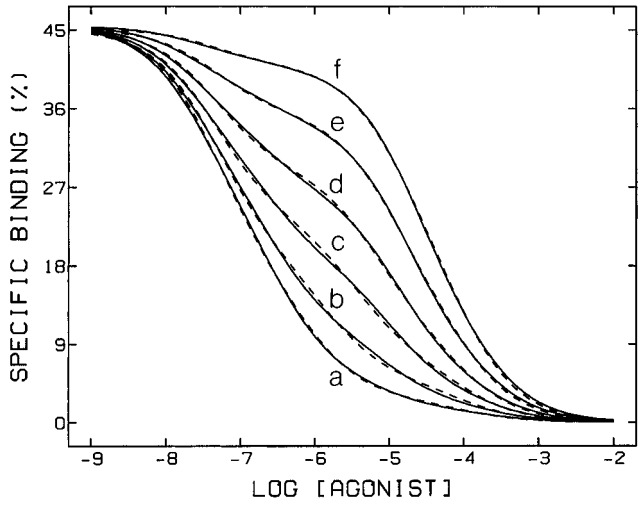

FIGURE 9: Effect of K_{RT} on binding to R and T in Scheme 3. The solid lines were simulated according to Scheme 3 at different values of K_{RT}, and the dashed lines illustrate the best fit of Scheme 1 (eq 4, n = 3) to the simulated data. Further details are described in Table 5. Deviations between the simulated and fitted curves arise primarily from the inability of Scheme 1 to mimic Scheme 3 at the parametric values selected for the latter. Restrictions on K_{A1} and K_{A3} in Scheme 1 affect the positions of the fitted curves by less than a line width. The abscissa shows the free concentration of the unlabeled ligand, and values plotted on the ordinate represent binding of the radioligand relative to the total concentration of sites taken as 100.

The effect of shifting the equilibrium between R and T is illustrated in Figure 9, where the solid lines were simulated at the values of K_{RT} listed in Table 5. Curves a and f represent the limits when the receptors are wholly in the R state ($-\log K_{RT} < -3$) or the T state ($-\log K_{RT} > +3$), respectively. The dashed lines represent the best fit of Scheme 1 to the simulated data, and the corresponding values of K_{Aj} and F_j are listed in Table 5. In this example, a decrease in K_{RT} emerges as an apparent interconversion of sites from higher to lower affinity in a system that reveals three states differentiated by agonists. There is a concomitant increase in the value of K_{Aj} at the sites of medium affinity with little or no change in that at the sites of high or low affinity. The curves in Figure 9 approximate the binding patterns obtained for M_2 muscarinic receptors in the present investigation (*cf.* Table 2, Figure 4A−C), but the overall pattern is typical of G protein-linked receptors in general. β-Adrenergic receptors reveal only two classes of sites [*e.g.*, Kent *et al.* (1980)], perhaps signaling a dimer (Hebert *et al.*, 1996), while receptors that inhibit adenylate cyclase often reveal the more complex patterns expected of larger oligomers. M_2 muscarinic receptors, α_2 adrenergic receptors, and D_2 dopamine receptors all have been reported to exhibit three classes of sites [*e.g.*, Mattera *et al.* (1985), Wong *et al.* (1986), Neubig *et al.* (1988), and Wreggett and Seeman (1984)].

The pattern in Figure 9 is obtained when half of the sites are functionally inaccessible to the radioligand (*i.e.*, −log

Table 5: Parametric Values for the Simulations in Figure 9[a]

	Scheme 3[b]	Scheme 1[c]			
curve	$-\log K_{RT}$	$-\log K_{A2}$	F_1	F_2	F_3
a	−6.0	7.171	0.613	0.328	0.059
b	−0.9	6.870	0.571	0.323	0.106
c	−0.4	6.477	0.484	0.358	0.158
d	0.0	6.187	0.360	0.421	0.219
e	0.5	5.991	0.216	0.465	0.319
f	6.0	5.873	0.093	0.446	0.461

[a] Data were simulated according to Scheme 3 with the values of K_{RT} listed in the table; other parameters are listed in footnote *b* below. The parametric values listed for Scheme 1 represent best fits of eq 4 ($n = 3$) to the simulated data. The value of $[P]_b$ was calculated with respect to the free concentrations of A and P, both for the simulations in terms of Scheme 3 (*cf.* eq 5.3) and for the analysis in terms of Scheme 1. [b] The values of other parameters are common to all curves. Those determined wholly or in part by the agonist are as follows: $-\log K_{AR} = 7.722$, $-\log a_{R2} = -0.176$, $-\log a_{R3} = -2.212$, $-\log a_{R4} = -1.051$, $-\log c_{R2} = 0.115$, $-\log c_{R3} = -1.674$, $-\log c_{R4} = -0.308$, $-\log K_{AT} = 8.084$, $-\log a_{T2} = -1.607$, $-\log a_{T3} = -0.959$, $-\log a_{T4} = -0.873$, $-\log c_{T2} = -1.011$, $-\log c_{T3} = 0.234$, $-\log c_{T4} = 0.152$. The values of a_{Rj} and a_{Tj} were selected such that the total cooperativity associated with ligand A was equal in R and T (*i.e.*, $a_{R2}a_{R3}a_{R4} = a_{T2}a_{T3}a_{T4}$). The two states of the receptor were assumed to be identical with respect to the radioligand (*i.e.*, R ≡ T), which was entered at a concentration of 1 nM; parameters unique to the radioligand were set to yield a Hill coefficient of 1 and an apparent affinity of 0.1 nM for binding to half of the sites, with the balance rendered functionally inaccessible through negative cooperativity (*i.e.*, $-\log K_P = 9.699$, $-\log p_2 = -0.176$, $-\log p_3 = -4.0$, $-\log p_4 = -0.176$). The value of $n[R]_t$ is 100. [c] The value of $-\log K_{Pj}$ was fixed at 10 for all three classes of sites. The values of $-\log K_{A1}$, $-\log K_{A3}$, and $[R]_t$ were common to all of the curves (*cf.* Table 2), and the fitted estimates are 8.375, 5.064, and 49.99, respectively.

$p_3 = -4.0$) and 91% of the balance are labeled in the absence of agonist. At higher levels of occupancy, similar behavior requires more than two states of the vacant receptor if the general approach represented by R and T in Scheme 3 is to be retained. The possibility of at least three states is consistent with evidence that muscarinic receptors are associated with more than one equivalent of G protein. Guanyl nucleotides have revealed multiple affinities when binding to receptor-linked G proteins labeled by [^{35}S]GTPγS [*e.g.*, Tota *et al.* (1987), Chidiac and Wells (1992), and Green *et al.* (1997)]; similarly, GMP-PNP, GTPγS, and GDP were found to be multiphasic in their effect on the binding of carbachol and *N*-[^{3}H]methylscopolamine to M_2 receptors, and GDP revealed a Hill coefficient of 1.4 (Figure 2). If the receptor is associated with multiple equivalents of G protein arranged in a cooperative array (Chidiac and Wells, 1992), each level of occupancy by the nucleotide may correspond to a different state of the receptor.

General Implications of Cooperativity. Scheme 3 and related models are intrinsically complex [*e.g.*, Eigen (1967)]. Their success is due in part to the comparatively large number of parameters, but they are implicated for more than their complexity alone. Cooperativity emerges in a model-independent manner, since the binding properties of purified M_2 receptors are inconsistent with the notion of mutually independent sites (Wreggett and Wells, 1995); similarly, cooperativity is implied by the complementary binding properties of receptor-linked G proteins (Chidiac and Wells, 1992). The complexity of Scheme 3 nevertheless leads to concern over its considerable scope. G protein-linked receptors are strikingly consistent in their binding properties, almost invariably yielding mechanistically ambiguous patterns similar to those reported here (*e.g.*, Figure 4). Oxotremorine-M has been found to increase the binding of [^{3}H]AF-DX 384 to purified M_2 receptors (Wreggett and Wells, 1995), but unrestricted cooperativity in a tetravalent receptor can predict much more extravagant effects that are seldom, if ever, reported.

The conformity of observed behavior suggests that many of the parameters of Scheme 3 are constrained, perhaps by the structure of the presumed oligomer represented by R and T. Such constraints also are implied by the observed correlations between efficacy and the multiple states of affinity revealed in binding assays [*e.g.*, Birdsall *et al.* (1977), Kent *et al.* (1980), Ehlert (1985), Evans *et al.* (1985), and Potter and Ferrendelli (1989)]. In the context of Scheme 3 and related models, multiple affinities arise in part from cooperativity between the agonist and the radiolabeled antagonist; in contrast, efficacy and intrinsic activity generally are measured in the absence of antagonist. It follows that cooperativity between successive equivalents of the agonist (a_j) may be related to cooperativity between the agonist and the radioligand (c_j). Such a possibility is supported by the observation that efficacy or intrinsic activity is correlated with both of the parameters that define the binding patterns of muscarinic or β-adrenergic agonists in terms of Scheme 1: namely, the ratio of affinities for the two states of the receptor and the apparent fraction of sites in one state or the other (Kent *et al.*, 1980; Evans *et al.*, 1985).

Cooperativity in the binding of agonists and guanyl nucleotides implies that signaling proceeds via oligomeric arrays of receptors on the one hand and G proteins on the other; moreover, the allosteric interactions between agonists and guanyl nucleotides appear to derive largely from changes induced by one ligand in the degree of cooperativity associated with the binding of the other. Amplification in such a system would depend upon the relative size of the two arrays and upon the extent to which the effect of the agonist is propagated throughout the array of G proteins. Capacities estimated from data on the binding of [^{35}S]GTPγS suggest that the number of receptor-sensitive G proteins is at least 20 times the number of receptors (Chidiac and Wells, 1992). That analysis was based on a dimer, but the disproportionate numbers raise the possibility that the oligomer of G proteins is much larger. Studies on the hydrodynamic properties of G proteins have suggested that the native structure is a multimer comparable in size to cross-linked tubulin (Coulter and Rodbell, 1992; Jahangeer and Rodbell, 1993).

The oligomer implied by Schemes 2 and 3 retains or appears to retain its structural integrity under the conditions of a binding assay: either there is no dissociation into constituent subunits or dissociated monomers do not exchange with those in a pool. Processes such as ligand-regulated oligomerization represent potential extensions to the model, and it has been suggested that agonists regulate the dimerization of m2 muscarinic and β_2-adrenergic receptors (Hirschberg and Schimerlik, 1994; Hebert *et al.*, 1996). Such extensions apparently are not required by the present data. Also, ligand-regulated oligomerization is difficult to reconcile with the evidence for a cooperative tetramer at picomolar concentrations of purified M_2 receptor in solution (Wreggett and Wells, 1995).

Oligomeric arrays of receptors and G proteins raise the possibility that one or both are heterogeneous. A heterooligomer of G proteins is suggested by the observation that α subunits of both G_o and G_i associate with cardiac muscarinic receptors from the same membranes (Matesic *et al.*, 1991; Wreggett and Wells, 1995). Heterooligomers of G protein-linked receptors can occur in experimentally contrived systems (Maggio *et al.*, 1993, 1996), and they might account for phenomena such as the reported interaction between D_1 and D_2 receptors in the striatum and anterior pituitary (Seeman *et al.*, 1989). Mixed oligomers of ionophoric glutamate receptors appear to occur *in vivo* (Wenthold *et al.*, 1996), and such a possibility broadens the scope for regulation and pharmacological selectivity in G protein-mediated systems.

ACKNOWLEDGMENT

We are grateful to Dr. Keith A. Wreggett for helpful comments on the manuscript, to Norman Pyo for discussions regarding the effects of alkylation with propylbenzilylcholine mustard, and to Dr. Franco Taverna for the drawings of Schemes 1−3. We thankfully acknowledge Adela Vigor and Maria Dekker for assistance with the binding assays.

REFERENCES

Adair, G. S. (1925) *J. Biol. Chem. 63*, 493−545.
Bennett, N., & Dupont, Y. (1985) *J. Biol. Chem. 260*, 4156−4168.
Birdsall, N. J. M., Burgen, A. S. V., & Hulme, E. C. (1977) *Adv. Behav. Biol. 24*, 25−33.
Birnbaumer, L., Abramowitz, J., & Brown, A. M. (1990) *Biochim. Biophys. Acta 1031*, 163−224.
Bokoch, G. M., Katada, T., Northup, J. K., Ui, M., & Gilman, A. G. (1984) *J. Biol. Chem. 259*, 3560−3567.
Bond, R. A., Leff, P., Johnson, T. D., Milano, C. A., Rockman, H. A., McMinn, T. R., Apparsundaram, S., Hyek, M. F., Kenakin, T. P., Allen, L. F., & Lefkowitz, R. J. (1995) *Nature 374*, 272−276.
Boyer, J. L., Martinez-Carcamo, M., Monroy-Sanchez, J. A., Posadas, C., & Garcia-Sainz, J. A. (1986) *Biochem. Biophys. Res. Commun. 134*, 172−177.
Brown, J. H., & Goldstein, D. (1986) *J. Pharmacol. Expt. Ther. 238*, 580−586.
Burgisser, E., De Lean, A., & Lefkowitz, R. J. (1982) *Proc. Natl. Acad. Sci. U.S.A. 79*, 1732−1736.
Chidiac, P., & Wells, J. W. (1992) *Biochemistry 31*, 10908−10921.
Chidiac, P., Nagy, A., Sole, M. J., & Wells, J. W. (1991) *J. Mol. Cell. Cardiol. 23*, 1255−1269.
Chidiac, P., Hebert, T. E., Valiquette, M., Dennis, M., & Bouvier, M. (1994) *Mol. Pharmacol. 45*, 490−499.
Costa, T., & Herz, A. (1989) *Proc. Natl. Acad. Sci. U.S.A. 86*, 7321−7325.
Coulter, S., & Rodbell, M. (1992) *Proc. Natl. Acad. Sci. U.S.A. 89*, 5842−5846.
Deighton, N. M., Motomura, S., Borquez, D., Zerkowski, H.-R., Doetsch, N., & Brodde, O.-E. (1990) *Naunyn-Schmiedeberg's Arch. Pharmacol. 341*, 14−21.
De Lean, A., Stadel, J. M., & Lefkowitz, R. J. (1980) *J. Biol. Chem. 255*, 7108−7117.
Ehlert, F. J. (1985) *Mol. Pharmacol. 28*, 410−421.
Ehlert, F. J., & Rathbun, B. E. (1990) *Mol. Pharmacol. 38*, 148−158.
Eigen, M. (1967) in *Fast Reactions and Primary Processes in Chemical Kinetics* (Claesson, S., Ed.) pp 333−369, Almquist and Wiksell, Stockholm.
Evans, T., Hepler, J. R., Masters, S. B., Brown, J. H., & Harden, T. K. (1985) *Biochem. J. 232*, 751−757.
Gilman, A. G. (1987) *Annu. Rev. Biochem. 56*, 615−649.
Graeser, D., & Neubig, R. R. (1993) *Mol. Pharmacol. 43*, 434−443.
Green, M. A., Chidiac, P., & Wells, J. W. (1997) *Biochemistry 36*, 7380−7394.
Hebert, T. E., Moffett, S., Morello, J.-P., Loisel, T. P., Bichet, D. G., Barret, C., & Bouvier, M. (1996) *J. Biol. Chem. 271*, 16384−16392.
Henis, Y. I., & Sokolovsky, M. (1983) *Mol. Pharmacol. 24*, 357−365.
Hilf, G., & Jakobs, K. H. (1992) *Eur. J. Pharmacol. 225*, 245−252.
Hilf, G., Gierschik, P., & Jakobs, K. H. (1989) *Eur. J. Biochem. 186*, 725−731.
Hirschberg, B. T., & Schimerlik, M. I. (1994) *J. Biol. Chem. 269*, 26127−26135.
Hulme, E. C., Berrie, C. P., Birdsall, N. J. M., & Burgen, A. S. V. (1981) *Eur. J. Pharmacol. 73*, 137−142.
Hulme, E. C., Birdsall, N. J. M., & Buckley, N. J. (1990) *Annu. Rev. Pharmacol. Toxicol. 30*, 633−673.
Ikegaya, T., Nishiyama, T., Haga, K., Haga, T., Ichiyama, A., Kobayashi, A., & Yamazaki, N. (1990) *J. Mol. Cell. Cardiol. 22*, 343−351.
Jahangeer, S., & Rodbell, M. (1993) *Proc. Natl. Acad. Sci. U.S.A. 90*, 8782−8786.
Kent, R. S., De Lean, A., & Lefkowitz, R. J. (1980) *Mol. Pharmacol. 17*, 14−23.
Kjelsberg, M. A., Cottecchia, S., Ostrowski, J., Caron, M. G., & Lefkowitz, R. J. (1992) *J. Biol. Chem. 267*, 1430−1433.
Koshland, D. E., Nemethy, G., & Filmer, D. (1966) *Biochemistry 5*, 365−385.
Lad, P. M., Neilsen, T. B., Preston, M. S., & Rodbell, M. (1980) *J. Biol. Chem. 255*, 988−995.
Lee, T. W. T., Sole, M. J., & Wells, J. W. (1986) *Biochemistry 25*, 7009−7020.
Leff, P. (1995) *Trends Pharmacol. Sci. 16*, 89−97.
Luetje, C. W., Brunwell, C., Norman, M. G., Peterson, G. L., Schimerlik, M. I., & Nathanson, N. M. (1987) *Biochemistry 26*, 6892−6896.
Maeda, A., Kubo, T., Mishina, M., & Numa, S. (1988) *FEBS Lett. 239*, 339−342.
Maggio, R., Vogel, Z., & Wess, J. (1993) *Proc. Natl. Acad. Sci. U.S.A. 90*, 3103−3107.
Maggio, R., Barbier, P., Fornai, F., & Corsini, G. U. (1996) *J. Biol. Chem. 271*, 31055−31060.
Marquardt, D. W. (1963) *J. Soc. Ind. Appl. Math. 2*, 431−441.
Matesic, D. F., Manning, D. R., & Luthin, G. R. (1991) *Mol. Pharmacol. 40*, 347−353.
Mattera, R., Pitts, B. J. R., Entman, M. L., & Birnbaumer, L. (1985) *J. Biol. Chem. 260*, 7410−7421.
Monod, J., Wyman, J., & Changeux, J.-P. (1965) *J. Mol. Biol. 12*, 88−118.
Munson, P. J., & Rodbard, D. (1980) *Anal. Biochem. 107*, 220−239.
Neubig, R. R., Gantzos, R. D., & Thomsen, W. J. (1988) *Biochemistry 27*, 2374−2384.
Peralta, E. G., Winslow, J. W., Peterson, G. L., Smith, D. H., Ashkenazi, A., Ramachandran, J., Schimerlik, M. I., & Capon, D. J. (1987) *Science 236*, 600−605.
Potter, L. T., & Ferrendelli, C. A. (1989) *J. Pharmacol. Expt. Ther. 248*, 974−978.
Pyo, N., & Wells, J. W. (1996) *Soc. Neurosci. Abstr. 22*, 1758.
Schütz, W., & Freissmuth, M. (1992) *Trends Pharmacol. Sci. 13*, 376−380.
Seeman, P., Niznik, H. B., Guan, H.-C., Booth, G., & Ulpian, C. (1989) *Proc. Natl. Acad. Sci. U.S.A. 86*, 10156−10160.
Sinkins, W. G., & Wells, J. W. (1993) *Mol. Pharmacol. 43*, 583−594.
Sinkins, W. G., Kandel, M., Kandel, S. I., Schunack, W., & Wells, J. W. (1993) *Mol. Pharmacol. 43*, 569−582.
Tobler, H. J., & Engel, G. (1983) *Naunyn-Schmiedeberg's Arch. Pharmacol. 322*, 183−192.
Tokaji, Z. (1993) *Biophys. J. 65*, 1130−1134.
Tota, M. R., Kahler, K. R., & Schimerlik, M. I. (1987) *Biochemistry 26*, 8175−8182.
Watson, M., Roeske, W. R., & Yamamura, H. I. (1986a) *J. Pharmacol. Expt. Ther. 237*, 419−427.

Watson, M., Yamamura, H. I., & Roeske, W. R. (1986b) *J. Pharmacol. Expt. Ther. 237*, 411−418.

Wells, J. W. (1992) in *Receptor-Ligand Interactions. A Practical Approach* (Hulme, E. C., Ed.) pp 289−395, Oxford University Press, Oxford, U.K.

Wenthold, R. J., Petralia, R. S., Blahos, J., & Niedzielski, A. S. (1996) *J. Neurosci. 16*, 1982−1989.

Wong, H.-M. S., Sole, M. J., & Wells, J. W. (1986) *Biochemistry 25*, 6995−7008.

Wreggett, K. A. (1987) *Biochem. Biophys. Res. Commun. 147*, 1070−1076.

Wreggett, K. A., & De Lean, A. (1984) *Mol. Pharmacol. 26*, 214−227.

Wreggett, K. A., & Seeman, P. (1984) *Mol. Pharmacol. 25*, 10−17.

Wreggett, K. A., & Wells, J. W. (1995) *J. Biol. Chem. 270*, 22488−22499.

BI961939T